DAFTAR PUSTAKA

Abbas, S., 2016. Konservasi nyamplung (*Calophyllum inophylum* L.) di kawasan pesisir Pantai Afetaduma Kecamatan Pulau Ternate Kota Ternate. Proceedings Of The International Conference On University-Community Engagement: 91-116. Universitas Islam Negeri Sunan Ampel.

Abdellah, M.H., Scholes, C.A., Liu, L., dan Kentish, S.E., 2020. Efficient degumming of crude canola oil using ultrafiltration membranes and bio-derived solvents. *Innov. Food Sci. Emerg. Technol.,* 59: 102274.

Abdullah, S.H.Y.S., Hanapi, N.H.M., Azid, A., Umar, R., Juahir, H., Khatoon, H., dan Endut, A., 2017. A review of biomass-derived heterogeneous catalyst for a sustainable biodiesel production. *Renew. Sustain. Energy Rev.,* 70: 1040-1051.

Abukhadra, M.R., Ibrahim, S.M., Yakout, S.M., El-Zaidy, M.E., dan Abdeltawab, A.A., 2019. Synthesis of Na^+ trapped bentonite/zeolite-P composite as a novel catalyst for effective production of biodiesel from palm oil; Effect of ultrasonic irradiation and mechanism. *Energy Conver. Manage.,* 196: 739-750.

Adenuga, A.A., Idowu, O.O., dan Oyekunle, J.A.O., 2020. Synthesis of quality biodiesel from *Calophyllum inophylum* kernels through reactive extraction method: Optimization of process parameters and characterization of the products. *Renew. Energy,* 145: 2530-2537.

Adepoju, T.F., 2021. Synthesis of biodiesel from *Annona muricata – Calophyllum inophylum* oil blends using calcined waste wood ash as a heterogeneous base catalyst. *MethodsX,* 8: 1-12.

Ahda, M., Sutarno, S., and Kunarti, E., 2013. Sintesis silika MCM-41 dan uji kapasitas adsorpsi terhadap metilen biru. *Pharmaciana,* 3(1): 1-8.

Ahmed, R., dan Huddersman, K., 2022. Review of biodiesel production by the esterification of wastewater containing fats oils and grease (FOGs). *J. Ind. Eng. Chem.,* 110: 1-14.

Al-Saadi, A., Mathan, B., dan He, Y., 2020. Biodiesel production via simultaneous transesterification and esterification reactions over SrO–ZnO/Al_2O_3 as a bifunctional catalyst using high acidic waste cooking oil. *Chem. Eng. Res. Des.,* 162: 238-248.

Albuquerque, M.C.G., Jiménez-Urbistondo, I., Santamaría-González, J., Mérida-Robles, J.M., Moreno-Tost, R., Rodríguez-Castellón, E., Jiménez-López, A., Azevedo, D.C.S., Cavalcante Jr, C.L., dan Maireles-Torres, P., 2008. CaO supported on mesoporous silicas as basic catalysts for transesterification reactions. *Appl. Catal. A: Gen.,* 334(1-2): 35-43.

Alothman, Z.A., 2012. A review: Fundamental aspects of silicate mesoporous materials. *Materials,* 5(12): 2874-2902.

Alvear-Daza, J.J., Pasquale, G.A., Rengifo-Herrera, J.A., Romanelli, G.P., dan Pizzio, L.R., 2021. Mesoporous activated carbon from sunflower shells modified with sulfonic acid groups as solid acid catalyst for itaconic acid esterification. *Catal. Today,* 372: 51-58.

Amin, A., Gadallah, A., El Morsi, A.K., El-Ibiari, N.N., dan El-Diwani, G.I., 2016. Experimental and empirical study of diesel and castor biodiesel blending effect, on kinematic viscosity, density and calorific value. *Egypt. J. Pet.,* 25(4): 509-514.

Ananda, A., dan Aini, S., 2021. Sintesis silika mesopori menggunakan bahan dasar Na_2SiO_3 yang dihasilkan dari pasir silika dengan metoda sol-gel. *Periodic,* 10(1): 37-39.

Aniya, V., Kumari, A., De, D., Vidya, D., Swapna, V., Thella, P.K., dan Satyavathi, B., 2018. Translation of lignocellulosic waste to mesoporous solid acid catalyst and its efficacy in esterification of volatile fatty acid. *Microporous Mesoporous Mater.,* 264: 198-207.

Aparamarta, H.W., Gunawan, S., Husin, H., Azhar, B., dan Tri Aditya, H., 2020. The effect of high oleic and linoleic fatty acid composition for quality and economical of biodiesel from crude *Calophyllum inophylum* oil (CCIO) with microwave-assisted extraction (MAE), batchwise solvent extraction (BSE), and combination of MAE–BSE methods. *Energy Rep.,* 6: 3240-3248.

Arumugam, A., dan Ponnusami, V., 2015. Optimization of recovery of silica from sugarcane leaf ash and Ca/SBA-15 solid base for transesterification of *Calophyllum inophylum* oil. *J. Sol-Gel Sci. Technol.,* 74(1): 132-142.

Arumugam, A., dan Ponnusami, V., 2019. Biodiesel production from *Calophyllum inophylum* oil a potential non-edible feedstock: An overview. *Renew. Energy,* 131: 459-471.

Arumugam, A., Senthamizhan, S.G., Ponnusami, V., dan Sudalai, S., 2018. Production and optimization of polyhydroxyalkanoates from non-edible *Calophyllum inophylum* oil using *Cupriavidus necator*. *Int. J. Biol. Macromol.,* 112: 598-607.

Ashwath, N., Nam, H., dan Capareda, S.C. 2018. Optimising pyrolysis conditions for thermal conversion of beauty leaf tree (*Calophyllum inophylum* L.) press cake. In application of thermo-fluid processes in energy systems: Key issues and recent developments for a sustainable future. M.M.K. Khan, A.A. Chowdhury, and N.M.S. Hassan, eds. Pp. 267-280. Singapore: Springer Singapore.

Askin, O.O., Askin, B., Bakanoğullari, G.B., dan Culum, S., 2018. Ülkemġz ġçġn farkli bġr yağ kaynaği: Pġrġnç kepeğġ yaği. *Kirklareli University Journal of Engineering and Science,* 4(1): 112-123.

Atabani, A.E., Silitonga, A.S., Ong, H.C., Mahlia, T.M.I., Masjuki, H.H., Badruddin, I.A., dan Fayaz, H., 2013. Non-edible vegetable oils: A critical evaluation of oil extraction, fatty acid compositions, biodiesel production, characteristics, engine performance and emissions production. *Renew. Sustain. Energy Rev.,* 18: 211-245.

Ayodele, O.O., dan Dawodu, F.A., 2014. Production of biodiesel from *Calophyllum inophylum* oil using a cellulose-derived catalyst. *Biomass Bioenergy,* 70: 239-248.

Baig, A., and Ng, F.T.T., 2010. A single-step solid acid-catalyzed process for the production of biodiesel from high free fatty acid feedstocks. *Energy Fuels,* 24(9): 4712-4720.

Balajii, M., dan Niju, S., 2020. Banana peduncle – A green and renewable heterogeneous base catalyst for biodiesel production from *Ceiba pentandra* oil. *Renew. Energy,* 146: 2255-2269.

Bandyopadhyay, M., Tsunoji, N., dan Sano, T., 2017. Mesoporous MCM-48 immobilized with aminopropyltriethoxysilane: A potential catalyst for transesterification of triacetin. *Catal. Lett.,* 147(4): 1040-1050.

Baroi, C., dan Dalai, A.K., 2013. Simultaneous esterification, transesterification and chlorophyll removal from green seed canola oil using solid acid catalysts. *Catal. Today* 207: 74-85.

Beck, J.S., Vartuli, J.C., Roth, W.J., Leonowicz, M.E., Kresge, C.T., Schmitt, K.D., Chu, C.T.-W., Olson, D.H., Sheppard, E.W., McCullen, S.B., Higgins, J.B., dan Schlenkert, J.L., 1992. A new family of mesoporous molecular sieves prepared with liquid crystal templates. *J. Am. Chem. Soc.,* 114(27): 10834-10843.

Bet-Moushoul, E., Farhadi, K., Mansourpanah, Y., Molaie, R., Forough, M., dan Nikbakht, A.M., 2016. Development of novel Ag/bauxite nanocomposite as a heterogeneous catalyst for biodiesel production. *Renew. Energy,* 92: 12-21.

Bhuiya, M., Rasul, M., Khan, M., dan Ashwath, N., 2019. Performance and emission characteristics of a compression ignition (CI) engine operated with beauty leaf biodiesel. *Energy Procedia,* 160: 641-647.

Bhuiya, M.M.K., Rasul, M., Khan, M., Ashwath, N., dan Mofijur, M., 2020. Comparison of oil extraction between screw press and solvent (n-hexane) extraction technique from beauty leaf (*Calophyllum inophylum* L.) feedstock. *Ind. Crops Prod.,* 144. 112024.

Bhuiya, M.M.K., Rasul, M.G., Khan, M.M.K., Ashwath, N., dan Azad, A.K., 2016. Prospects of 2nd generation biodiesel as a sustainable fuel—Part: 1 selection of feedstocks, oil extraction techniques and conversion technologies. *Renew. Sustain. Energy Rev.,* 55: 1109-1128.

Bilgin, A., Gülüm, M., Koyuncuoglu, İ., Nac, E., dan Cakmak, A., 2015. Determination of transesterification reaction parameters giving the lowest viscosity waste cooking oil biodiesel. *Procedia Soc. Behav. Sci.,* 195: 2492-2500.

Bilton, M.W. 2012. Nanoparticulate hydroxyapatite and calcium-based CO_2 sorbents, School of Process, Environmental and Materials Engineering, University of Leeds Institute for Materials Research, United Kingdom.

Blin, J.L., Herrier, G., Otjacques, C., dan Su, B.-L. 2000. New way to synthesize MCM-41 and MCM-48 materials with tailored pore sizes. *In* Studies in Surface Science and Catalysis. A. Sayari and M. Jaroniec, eds. Pp. 57-66: Elsevier.

Cabrera-Munguia, D.A., González, H., Gutiérrez-Alejandre, A., Rico, J.L., Huirache-Acuña, R., Maya-Yescas, R., dan del Río, R.E., 2017. Heterogeneous acid conversion of a tricaprylin-palmitic acid mixture over Al-SBA-15 catalysts: Reaction study for biodiesel synthesis. *Catalysis Today,* 282, Part 2: 195-203.

Cao, M., Peng, L., Xie, Q., Xing, K., Lu, M., dan Ji, J., 2021. Sulfonated Sargassum horneri carbon as solid acid catalyst to produce biodiesel via esterification. *Bioresour Technol,* 324: 124614.

Cara, C., Rombi, E., Mameli, V., Ardu, A., Sanna Angotzi, M., Niznansky, D., Musinu, A., dan Cannas, C., 2018. γ-Fe_2O_3-M41S sorbents for H_2S removal: Effect of different porous structures and silica wall thickness. *J. Phys. Chem. C.,* 122(23): 12231-12242.

Carmo, J.A.C., Souza, D.L.K.C., Costa, D.C.E.F., Longo, E., Zamian, J.R., dan Rocha, D.F.G.N., 2009. Production of biodiesel by esterification of palmitic acido over mesoporous aluminosilicate Al-MCM-41. *Fuel,* 88: 461-468.

Chavan, S.B., Kumbhar, R.R., dan Deshmukh, R.B., 2013. *Callophyllum inophyllum* L. ("Honne") oil, a source for biodiesel production. *Res. J. Chem. Sci.,* 3(11): 24-31.

Chen, W.-K., Tseng, H.-H., Wei, M.-C., Su, E.-C., dan Chiu, I.C., 2014. Transesterification of canola oil as biodiesel over Na/Zr-SBA-15 catalysts: Effect of zirconium content. *Int. J. Hydrog. Energy,* 39(34): 19555-19562.

Chum-in, T., Sudaprasert, K., Phankosol, S., Lilitchan, S., Aryusuk, K., dan Krisnangkura, K., 2016. Gibbs energy additivity approaches to QSPR in modeling of high pressure dynamic viscosity of FAME and biodiesel. *J. of Mol. Liq.,* 223: 1006-1012.

Chum-in, T., Sudaprasert, K., Phankosol, S., Lilitchan, S., Aryusuk, K., dan Krisnangkura, K., 2017. Gibbs energy additivity approaches to QSPR in modeling of high pressure density and kinematic viscosity of FAME and biodiesel. *Fuel Process. Technol.,* 156: 385-393.

Costa, E., Almeida, M.F., Alvim-Ferraz, M.d.C., dan Dias, J.M., 2018. Effect of Crambe abyssinica oil degumming in phosphorus concentration of refined oil and derived biodiesel. *Renew. Energy,* 124: 27-33.

Costa, J.A.S., de Jesus, R.A., Santos, D.O., Neris, J.B., Figueiredo, R.T., dan Paranhos, C.M., 2021. Synthesis, functionalization, and environmental application of silica-based mesoporous materials of the M41S and SBA-n families: A review. *J. of Environ. Chem. Eng.,* 9(3). 105259.

Dadhania, H., Raval, D., dan Dadhania, A., 2021. Magnetically separable heteropolyanion based ionic liquid as a heterogeneous catalyst for ultrasound mediated biodiesel production through esterification of fatty acids. *Fuel,* 296. 120673.

Dahdah, E., Estephane, J., Haydar, R., Youssef, Y., El Khoury, B., Gennequin, C., Aboukaïs, A., Abi-Aad, E., dan Aouad, S., 2020. Biodiesel production from refined sunflower oil over Ca–Mg–Al catalysts: Effect of the composition and the thermal treatment. *Renew. Energy,* 146: 1242-1248.

Damanik, N., Ong, H.C., Tong, C.W., Mahlia, T.M.I., dan Silitonga, A.S., 2018. A review on the engine performance and exhaust emission characteristics of diesel engines fueled with biodiesel blends. *Environ. Sci. Pollut. Res.,* 25(16): 15307-15325.

Dampang, S., Purwanti, E., Destyorini, F., Kurniawan, S.B.K., Abdullah, S.R.S., dan Imron, M., 2021. Analysis of optimum temperature and calcination time in the production of cao using seashells waste as $CaCO_3$ source. *J. Ecol. Eng.,* 22(5): 221-228.

de Almeida Andrade, M.R., Silva, C.B., Costa, T.K.O., de Barros Neto, E.L., dan Lavoie, J.-M., 2021. An experimental investigation on the effect of surfactant for the transesterification of soybean oil over eggshell-derived CaO catalysts. *Energy Convers. Manag.: X,* 11: 100094.

Dehghani, S., dan Haghighi, M., 2017. Sono-sulfated zirconia nanocatalyst supported on MCM-41 for Biodiesel Production from sunflower oil: Influence of ultrasound irradiation power on catalytic properties and performance. *ultrason. Sonochem.,* 35, Part A: 142-151.

Desanto, T. 2022. *In* Banyaknya Curah Hujan dan Hari Hujan/Number of Preticipatios and Rainy days 2016-2022: Badan Pusat Statistik Kabupaten Cilacap.

Dhawane, S.H., Kumar, T., dan Halder, G., 2016. Biodiesel synthesis from *Hevea brasiliensis* oil employing carbon supported heterogeneous catalyst: Optimization by Taguchi method. *Renew. Energy,* 89: 506-514.

Ding, Y., Zhao, C., Lia, Y., Ma, Z., dan Lv, X., 2018. Effect of calcination temperature on the structure and catalytic performance of the Cu-MCM-41 catalysts for the synthesis of dimethyl carbonate. *Quím. Nova,* 41(10): 1156-1161.

Efavi, J.K., Kanbogtah, D., Apalangya, V., Nyankson, E., Tiburu, E.K., Dodoo-Arhin, D., Onwona-Agyeman, B., dan Yaya, A., 2018. The effect of NaOH catalyst concentration and extraction time on the yield and properties of *Citrullus vulgaris* seed oil as a potential biodiesel feed stock. *S. Afr. J. Chem. Eng.,* 25: 98-102.

El-Hakam, S.A., Alshorifi, F.T., Salama, R.S., Gamal, S., El-Yazeed, W.S.A., Ibrahim, A.A., dan Ahmed, A.I., 2022. Application of nanostructured mesoporous silica/ bismuth vanadate composite catalysts for the degradation of methylene blue and brilliant green. *J. of Mater. Res. Technol.,* 18: 1963-1976.

Elma, M., Suhendra, S., dan Wahyuddin. 2016. Proses pembuatan biodiesel dari campuran minyak kelapa dan minyak jelantah. *J. Konversi,* 5(1): 8-17.

Elzanati, E., Abdallah, H., Farg, E., Ettouney, R.S., El-Rifai, M.A., dan 2018. Enhancing the esterification conversion using pervaporation. *J. Eng. Sci. Technol.,* 13(4): 990-1004.

Enggawati, E.R., dan Ediati, R., 2013. Pemanfaatan kulit telur ayam dan abu layang batubara sebagai katalis heterogen untuk reaksi transesterifikasi minyak nyamplung (*Calophyllum inophylum* Linn). *Jurnal Sains dan Seni ITS,* 2(1): 2337-3520.

Fadhil, A.B., Aziz, A.M., dan Al-Tamer, M.H., 2016. Biodiesel production from *Silybum marianum* L. seed oil with high FFA content using sulfonated carbon catalyst for esterification and base catalyst for transesterification. *Energy Con. Manag.,* 108: 255-265.

Fadhlullah, M., Widiyanto, S.N.B., dan Restiawaty, E., 2015. The potential of nyamplung (*Calophyllum inophylum* L.) seed oil as biodiesel feedstock: effect of seed moisture content and particle size on oil yield. *Energy Procedia,* 68:177-185

Falcaro, P., Bertolo, J.M., Innocenzi, P., Amenitsch, H., and Bearzotti, A., 2004. Ordered mesostructured silica films: Effect of pore surface on its sensing properties. *J. Solgel Sci. Technol.,* 32(1): 107-110.

Falowo, O.A., Apanisile, O.E., Aladelusi, A.O., Adeleke, A.E., Oke, M.A., Enamhanye, A., Latinwo, L.M., dan Betiku, E., 2021. Influence of nature of catalyst on biodiesel synthesis via irradiation-aided transesterification of waste cooking oil-honne seed oil blend: Modeling and optimization by Taguchi design method. *Energy Con. Manag. X,* 12. 100119.

Farooq, M., Ramli, A., Naeem, A., Mahmood, T., Ahmad, S., Humayun, M., dan Islam, M.G.U., 2018. Biodiesel production from date seed oil (*Phoenix dactylifera* L.) via egg shell derived heterogeneous catalyst. *Chem. Eng. Res. Des.,* 132: 644-651.

Fathy, M., Selim, H., dan Shahawy, A.E.L., 2020. Chitosan/MCM-48 nanocomposite as a potential adsorbent for removing phenol from aqueous solution. *RSC Adv.,* 10(39): 23417-23430.

Fenangad, D.B., Abon, J.E.O., Mabalot, P.E., dan Orge, R.F., 2015. Production of biodiesel from waste cooking oil using the cruzesterification process for rice farming operations. *Int. J. Sustain. Dev.,* 8(12): 25-31.

Filho, B.A.O., Barros, A.K.D., Labidi, S., Viegas, I.M.A., Marques, D.B., Romariz, A.R.S., de Sousa, R.M., Marques, A.L.B., dan Marques, E.P., 2015. Application of artificial neural networks to predict viscosity, iodine value and induction period of biodiesel focused on the study of oxidative stability. *Fuel,* 145: 127-135.

Ghaedi, H., and Zhao, M., 2022. Review on template removal techniques for synthesis of mesoporous silica materials. *Energy Fuels,* 36(5): 2424-2446.

Gholampour, N., Yusubov, M., dan Verpoort, F., 2016. Investigation of the preparation and catalytic activity of supported Mo, W, and Re oxides as heterogeneous catalysts in olefin metathesis. *Catal. Rev.,* 58: 1-44.

Goh, B.H.H., Ong, H.C., Chong, C.T., Chen, W.-H., Leong, K.Y., Tan, S.X., dan Lee, X.J., 2020. Ultrasonic assisted oil extraction and biodiesel synthesis of Spent Coffee Ground. *Fuel,* 261: 116121.

Gohain, M., Laskar, K., Paul, A.K., Daimary, N., Maharana, M., Goswami, I.K., Hazarika, A., Bora, U., dan Deka, D., 2020a. *Carica papaya* stem: A source of versatile heterogeneous catalyst for biodiesel production and C–C bond formation. *Renew. Energy,* 147: 541-555.

Gohain, M., Laskar, K., Phukon, H., Bora, U., Kalita, D., dan Deka, D., 2020b. Towards sustainable biodiesel and chemical production: Multifunctional use of heterogeneous catalyst from littered *Tectona grandis* leaves. *Waste Manag.,* 102: 212-221.

Gomez-Verjan, J., Gonzalez-Sanchez, I., Estrella-Parra, E., dan Reyes-Chilpa, R., 2015. Trends in the chemical and pharmacological research on the tropical trees *Calophyllum brasiliense* and *Calophyllum inophylum*, a global context. *Scientometrics,* 105(2): 1019-1030.

Granados, M.L., Poves, M.D.Z., Alonso, D.M., Mariscal, R., Galisteo, F.C., Moreno-Tost, R., Santamaría, J., dan Fierro, J.L.G., 2007. Biodiesel from sunflower oil by using activated calcium oxide. *Appl. Catal. B: Environ.,* 73(3-4): 317-326.

Gulum, M., Yesilyurt, M.K., dan Bilgin, A., 2020. The modeling and analysis of transesterification reaction conditions in the selection of optimal biodiesel yield and viscosity. *Environ. Sci. Pollu.t Res. Int.,* 27(10): 10351-10366.

Gunawidjaja, P.N., Mathew, R., Lo, A.Y., Izquierdo-Barba, I., Garcia, A., Arcos, D., Vallet-Regi, M., dan Eden, M., 2012. Local structures of mesoporous bioactive glasses and their surface alterations in vitro: inferences from solid-state nuclear magnetic resonance. *Philos. Trans. A Math. Phys. Eng. Sci.,* 370(1963): 1376-1399.

Hani, A., dan Rachman, E., 2016. Pertumbuhan tanaman nyamplung sampai umur 4 (empat) tahun pada tiga pola tanam dan dosis pupuk di lahan pantai berpasir Pangandaran, Jawa Barat. *J. P. K. Wallacea,* 5(2): 151-158.

Haryono, Natanael, C.L., Rukiah, dan Yulianti, Y.B., 2018. Kalsium oksida mikropartikel dari cangkang telur sebagai katalis pada sintesis biodiesel dari minyak goreng bekas. *J. Material Energi Indones.,* 8(1): 8-15.

Helwani, Z., Othman, M.R., Aziz, N., Kim, J., dan Fernando, W.J.N., 2009. Solid heterogeneous catalysts for transesterification of triglycerides with methanol: A review. *Appl. Catal. A : Gen.,* 363 1-10.

Hendra, D., Wibowo, S., Hastuti, N., dan Wibisono, H., 2016. Karakteristik biodiesel biji bintaro (*Cerbera manghas* L.) dengan proses modifikasi. *J. Penelit. Has. Hutan,* 34: 11-21.

Herlina, I., dan Safitra, E.R., 2018. Sintesis dan karakterisasi silika tersulfatasi dari sekam padi. *J. Rek. Pros.,* 12(1): 17-22.

Heryati, Y. 2007. Nyamplung, Departemen Kehutanan Badan Penelitian dan Pengembangan Kehutanan Pusat Penelitian dan Pengembangan Hutan Tanaman.

Hidayati, N., Ariyanto, T.S., dan Septiawan, H., 2017. Transesterifikasi minyak goreng bekas menjadi biodiesel dengan katalis kalsium oksida. *Jurnal Teknologi Bahan Alam,* 1(1): 1-5.

Hosseini, S.A., 2022. Nanocatalysts for biodiesel production. *Arab. J. Chem.,* 15(10).

How, H.G., Masjuki, H.H., Kalam, M.A., Teoh, Y.H., dan Chuah, H.G., 2018. Effect of *Calophyllum inophylum* biodiesel-diesel blends on combustion, performance, exhaust particulate matter and gaseous emissions in a multi-cylinder diesel engine. *Fuel,* 227: 154-164.

Huang, R., Cheng, J., Qiu, Y., Li, T., Zhou, J., dan Cen, K., 2015. Using renewable ethanol and isopropanol for lipid transesterification in wet microalgae cells to produce biodiesel with low crystallization temperature. *Energy Convers. Manag.,* 105: 791-797.

Ibrahim, H.G., Alshuiref, A.A., dan Maraie, A.A., 2015. Recycling of waste cooking oils (WCO) to biodiesel production. *J. Multidisciplinary Eng. Sci. Technol.,* 2(4): 721-725.

Ibrahim, S.M., dan Halim, S.A., 2021. Novel SnZr oxides nanomaterials synthesized by ultrasonic-assisted co-precipitation method: Application in biodiesel production and DFT study. *J. Mol. Liq.,* 339: 116652.

Jain, S. 2019. 17-The production of biodiesel using karanja (*Pongamia pinnata*) and jatropha (*Jatropha curcas*) oil. In biomass, biopolymer-based materials, and bioenergy. D. Verma, E. Fortunati, S. Jain, and X. Zhang, eds. Pp. 397-408: Woodhead Publishing.

Jamshidi, D., dan Sazegar, M.R., 2020. Antibacterial activity of a novel biocomposite chitosan/graphite based on zinc-grafted mesoporous silica nanoparticles. *Int. J. Nanomed.,* 15: 871-883.

Jarmolinska, S., Feliczak-Guzik, A., dan Nowak, I., 2020. Synthesis, characterization and use of mesoporous silicas of the following types SBA-1, SBA-2, HMM-1 and HMM-2. *Materials (Basel),* 13(19): 1-33.

Jauhari, M., Maryati, R., dan Khairani, K., 2018. Analisa Perbandingan Kualitas Biodiesel Dari Minyak Jelantah Berdasarkan Perbedaan Penggunaan Jenis Reaktor. *J. INTEKNA,* 18(1): 31-39.

Jayakumar, M., Karmegam, N., Gundupalli, M.P., Bizuneh Gebeyehu, K., Tessema Asfaw, B., Chang, S.W., Ravindran, B., dan Kumar Awasthi, M., 2021. Heterogeneous base catalysts: Synthesis and application for biodiesel production - A review. *Bioresour Technol,* 331: 125054.

Jeenpadiphat, S., Björk, E.M., Odén, M., dan Tungasmita, D.N., 2015. Propylsulfonic acid functionalized mesoporous silica catalysts for esterification of fatty acids. *J.Mol. Catal. A: Chem.,* 410: 253-259.

Jeevanantham, A.K., Nanthagopal, K., Ashok, B., Al-Muhtaseb, A.a.H., Thiyagarajan, S., Geo, V.E., Ong, H.C., dan Samuel, K.J., 2019. Impact of addition of two ether additives with high speed diesel - *Calophyllum inophylum* biodiesel blends on NO_x reduction in CI engine. *Energy,* 185: 39-54.

Jiao, T., Liu, X., dan Niu, J., 2016. Effects of sodium chloride on adsorption at different interfaces and aggregation behaviors of disulfonate gemini surfactants. *RSC Adv.,* 6(17): 13881-13889.

Joshi, G., Rawat, D.S., Lamba, B.Y., Bisht, K.K., Kumar, P., Kumar, N., dan Kumar, S., 2015. Transesterification of jatropha and karanja oils by using waste egg shell derived calcium based mixed metal oxides. *Energy Conver. Manag.,* 96: 258-267.

Jun, S., Kim, J.M., Ryoo, R., Ahn, Y.-S., dan Han, M.-H., 2000. Hydrothermal stability of MCM-48 improved by post-synthesis restructuring in salt solution. *Microporous Mesoporous Mater.,* 41(1): 119-127.

Juwono, H., Triyono, T., Sutarno, S., Wahyuni, E.T., Ulfin, I., dan Kurniawan, F., 2017. Production of biodiesel from seed oil of nyamplung (*Calophyllum inophylum*) by Al-MCM-41 and its performance in diesel engine. *Indones. J. Chem.,* 17(2): 316-321.

Karami, R., Hoseinpour, M., Rasul, M.G., Hassan, N.M.S., dan Khan, M.M.K., 2022. Exergy, energy, and emissions analyses of binary and ternary blends of seed waste biodiesel of tomato, papaya, and apricot in a diesel engine. *Energy Convers. Manag. X,* 16.

Kartika, D., dan Widyaningsih, S., 2012. Konsentrasi katalis dan suhu optimum pada reaksi esterifikasi menggunakan katalis zeolit alam aktif (ZAH) dalam pembuatan biodiesel dari minyak jelantah. *J. Natur Indones.,* 14(3): 219-226.

Kaur, M., Malhotra, R., dan Ali, A., 2018. Tungsten supported Ti/SiO_2 nanoflowers as reusable heterogeneous catalyst for biodiesel production. *Renew. Energy,* 116: 109-119.

Kesica, Z., Lukic, I., Zdujic, M., Liu, H., dan Skala, D., 2012. Mechanochemically synthesized CaO ZnO catalyst for biodiesel production. *Procedia Eng.,* 42: 1169-1178.

Khamidah, N., dan Darmawan, A.R.B., 2018. Viabilitas benih nyamplung (*Calophyllum inophylum* L.) dari biji yang telah di skarifikasi terhadap media tanam yang berbeda. *ZIRAA’AH,* 43(1): 104-110.

Kharnofa, T., Bahri, S., dan Yusnimar. 2016. Produksi biodiesel dari minyak nyamplung dengan katalis Ni/lempung. *Jom FTEKNIK,* 3(2): 1-6.

Kiggundu, N., and Jjagwe, J., 2021. Performance evaluation of a motorised palm oil extractor with quality assessment of the palm oil extracted in comparison with a manual vertical press. *J. Oil Palm Res.,* 33(1): 64-73.

Kirubakaran, M., dan Arul Mozhi Selvan, V., 2021. Experimental investigation on the effects of micro eggshell and nano-eggshell catalysts on biodiesel optimization from waste chicken fat. *Bioresour. Technol. Rep.,* 14: 100658.

Kolo, L. 2015. Penggunaan MCM-48-nCaO sebagai katalis pada reaksi transesterifikasi minyak biji nyamplung (*Calophyllum inophylum* L.) menjadi biodiesel. Tesis belum dipublikasi. Departemen Kimia. Universitas Hasanuddin. Makassar.

Kolo, L., Firdaus, dan Taba, P., 2015. The use of mcm-48-ncao as catalyst in esterification reaction of nyamplung seed oil (*Calophyllum inophylum* L.). *Indones. Chim. Acta,* 8(20): 1-10.

Kolo, L., Firdaus, Taba, P., Zakir, M., dan Soekamto, N.H., 2022. Selectivity of the new catalyst ZnO-MCM-48-CaO in esterification of *Calophyllum inophylum* oil. *A. E.,* 5(2): 217-229.

Kondamudi, N., Mohapatra, S.K., dan Misra, M., 2011. Quintinite as a bifunctional heterogeneous catalyst for biodiesel synthesis. *Appl. Catal. A: Gen.,* 393(1-2): 36-43.

Kouzu, M., dan Hidaka, J.-s., 2012. Transesterification of vegetable oil into biodiesel catalyzed by CaO: A review. *Fuel,* 93: 1-12.

Kresge, C.T., and Roth, W.J., 2013. The discovery of mesoporous molecular sieves from the twenty year perspective. *Chem. Soc. Rev.,* 42(9): 3663-70.

Kubota, Y., Ikeya, H., Sugi, Y., Yamada, T., dan Tatsumi, T., 2006. Organic-inorganic hybrid catalysts based on ordered porous structures for Michael reaction. *J. Mol. Catal. A : Chem.,* 249: 181-190.

Kulkarni, V., Jain, S., Khatri, F., dan Thulasi, V., 2014. Degumming of *Pongamia Pinnata* by acid and water degumming methods. *Int. J. Chemtech. Res.,* 6: 3969-3978.

Kumar, A., dan Sharma, S., 2011. Potential non-edible oil resources as biodiesel feedstock: an Indian perspective. *Renew. Sust. Energy Rev.,* 15: 1791-1800.

Kumar, S., dan Prasad, A., 2019. Environment friendly butyl ester biodiesel production from mahua oil: optimization and characterization. *SN Appl. Sci.,* 1(8): 872.

Kurniati, S., Soeparman, S., Setyo Yuwono, S., Hakim, L., dan Syam, S., 2019. A novel process for production of *Calophyllum inophylum* biodiesel with electromagnetic induction. *Energies,* 12(3): 1-21.

Lai, T.-L., Shu, Y.-Y., Lin, Y.-C., Chen, W.-N., dan Wang, C.-B., 2009. Rapid removal of organic template from SBA-15 with microwave assisted extraction. *Mater. Lett.,* 63(20): 1693-1695.

Lam, J., Huang, M., Tan, H., Mo, Z., Mai, Z., Wong, C., Sun, H., dan Shen, Z., 2011. Vibrational spectroscopy of low-k/ultra-low-k dielectric materials on patterned wafers. *Journal of Vacuum Science & Technology A: Vacuum, Surfaces, and Films,* 29: 051513-051513.

Lawan, I., Zhou, W., Idris, A.L., Jiang, Y., Zhang, M., Wang, L., dan Yuan, Z., 2020. Synthesis, properties and effects of a multi-functional biodiesel fuel additive. *Fuel Process.Technol.,* 198: 106228.

Lee, A.F., Bennett, J.A., Manayil, J.C., dan Wilson, K., 2014. Heterogeneous catalysis for sustainable biodiesel production via esterification and transesterification. *Chem. Soc. Rev.,* 43(22): 7887-7916.

Lee, A.F., dan Wilson, K., 2015. Recent developments in heterogeneous catalysis for the sustainable production of biodiesel. *Catal. Today,* 242: 3-18.

Leksono, B., Hendrati, R.L., Windyarini, E., dan Hasnah, T., 2014a. Variation in biofuel potential of twelve *Calopyllum Inophyllum* populations in Indonesia. *Indones. J. of Forestry Res.,* 1(2): 127-138.

Leksono, B., Windyarini, E., dan Hasnah, T.M., 2014b. Budidaya nyamplung (*Calophyllum inophylum* L.) untuk bioenergi dan prospek pemanfaatan lainnya. Kementerian Kehutanan, IPB Press, Bogor, Indonesia.

Li, X., Chen, W., Tang, Y., dan Li, L., 2018. Relationship between the structure of Fe-MCM-48 and its activity in catalytic ozonation for diclofenac mineralization. *Chemosphere,* 206: 615-621.

Lin, H.-P., and Mou, C.-Y., 2002. Salt effect in post-synthesis hydrothermal treatment of MCM-41. *Microporous Mesoporous Mater.,* 55(1): 69-80.

Lin, J., Zhao, B., Cao, Y., Xu, H., Ma, S., Guo, M., Qiao, D., dan Cao, Y., 2014. Rationally designed Fe-MCM-41 by protein size to enhance lipase immobilization, catalytic efficiency and performance. *Appl. Catal. A : Gen.,* 478: 175-185.

Liu, J., Nan, Y., Lawrence, L., dan Tavlarides. 2017. Continuous production of ethanol-based biodiesel under subcritical conditions employing trace amount of homogeneous catalysts. *Fuel,* 193: 187-196.

Liu, Y., Lv, M., Li, L., Yu, H., Wu, Q., Pang, J., Liu, Y., Xie, C., Yu, S., dan Liu, S., 2019. Synthesis of rosin methyl ester using PTSA/ZrO_2/Mo-MCM-41 mesoporous molecular sieves. *Catal. Lett.,* 149(7): 1911-1918.

Luo, S., Yao, J., Wang, R., Wang, L., Chen, X., Yu, D., dan Elfalleh, W., 2021. Effect of nickel modification on Ru–Ni/NaY catalyst structure and linoleic acid isomerization selectivity. *J. Food Meas. Charact.,* 15(6): 5584-5598.

Maddalena, R., Hall, C., dan Hamilton, A., 2019. Effect of silica particle size on the formation of calcium silicate hydrate [C-S-H] using thermal analysis. *Thermochim. Acta,* 672: 142-149.

Mahlia, T.M.I., Syazmi, Z.A.H.S., Mofijur, M., Abas, A.E.P., Bilad, M.R., Ong, H.C., dan Silitonga, A.S., 2020. Patent landscape review on biodiesel production: Technology updates. *Renew. Sustain. Energy Rev.,* 118: 109526.

Malhis, A.A., Arar, S.H., Fayyad, M.K., dan Hodali, H.A., 2017. Amino- and thiol-modified microporous silicalite-1 and mesoporous MCM-48 materials as potential effective adsorbents for Pb(II) in polluted aquatic systems. *Adsorpt. Sci. Technol.,* 36(1-2): 270-286.

Mallah, T.A., dan Sahito, A.R., 2020. Optimization of castor and neem biodiesel blends and development of empirical models to predicts its characteristics. *Fuel,* 262: 116341.

Manabe, K., Sun, X.-M., dan Kobayashi, S., 2001. Dehydration reactions in water. surfactant-type Brønsted acid-catalyzed direct esterification of carboxylic acids with alcohols in an emulsion system. *J. Am. Chem. Soc.,* 123(41): 10101-10102.

Mangoensoekarjo, S., and Semangun, H. 2003. Manajemen Agrobisnis Kelapa Sawit. Gadjah Mada University Press. Yogyakarta.

Manique, M.C., Lacerda, L.V., Alves, A.K., dan Bergmann, C.P., 2017. Biodiesel production using coal fly ash-derived sodalite as a heterogeneous catalyst. *Fuel,* 190: 268-273.

Manurung, J. 2010. Analisis sifat sifat fisika-kimia dan emisi gas buang dari biodiesel B10, B20 turunan minyak kacang tanah melalui proses transesterifikasi dengan katalis KOH. Tesis belum dipublikasi. Medan: Program Pascasarjana Fisika. Universitas Sumatera Utara.

Marinković, D.M., Stanković, M.V., Veličković, A.V., Avramović, J.M., Miladinović, M.R., Stamenković, O.O., Veljković, V.B., dan Jovanović, D.M., 2016. Calcium oxide as a promising heterogeneous catalyst for biodiesel production: Current state and perspectives. *Renew. Sustain. Energy Rev.,* 56: 1387-1408.

Markovskaya, D.V., Cherepanova, S.V., Gerasimov, E.Y., Zhurenok, A.V., Selivanova, A.V., Selishchev, D.S., dan Kozlova, E.A., 2020. The influence of the sacrificial agent nature on transformations of the $Zn(OH)_2$/Cd0.3Zn0.7S photocatalyst during hydrogen production under visible light. *RSC Adv.,* 10(3): 1341-1350.

Marso, T.M.M., Kalpage, C.S., dan Udugala-Ganehenege, M.Y., 2017. Metal modified graphene oxide composite catalyst for the production of biodiesel via pre-esterification of *Calophyllum inophylum* oil. *Fuel,* 199: 47-64.

Marwati, Taebe, B., Tandilolo, A., and Nur, S., 2021. Pengaruh Tempat Tumbuh dan Profil Kandungan Kimia Minyak Atsiri dari Rimpang Jahe Merah (Zingiber officinalle Linn. Var rubrum). *J. Sains Kes. ,* 3(2): 248-254.

Masteri-Farahani, M., Hosseini, M.-S., dan Forouzeshfar, N., 2020. Propyl-SO_3H functionalized graphene oxide as multipurpose solid acid catalyst for biodiesel synthesis and acid-catalyzed esterification and acetalization reactions. *Renew. Energy,* 151: 1092-1101.

Mlay, H., Katima, J.H.Y., dan Minja, R.J.A., 2014. Modifying plant oils for use as fuel in Rural Contexts Tanzania: Techno-economic analysis. *Open J. Model. Simul.,* 2(2): 43-56.

Mohamad, M., Ngadi, N., Wong, S.L., Jusoh, M., and Yahya, N.Y., 2017. Prediction of biodiesel yield during transesterification process using response surface methodology. *Fuel,* 190: 104-112

Mokri, N.A., Pei Ching, O., Mukhtar, H., dan Thiam Leng, C., 2019. Tailoring particle size and agglomeration state of mesoporous MCM-48 via optimisation of sol-gel silica process. *J. Phy. Sci.,* 30(1): 145-168.

Molinari, R., Lavorato, C., Mastropietro, T.F., Argurio, P., Drioli, E., and Poerio, T., 2016. Preparation of Pd-Loaded hierarchical FAU membranes and testing in acetophenone hydrogenation. *Molecules,* 21(3): 394.

Mousavi-Kamazani, M., Zinatloo-Ajabshir, S., dan Ghodrati, M., 2020. One-step sonochemical synthesis of $Zn(OH)_2/ZnV_3O_8$ nanostructures as a potent material in electrochemical hydrogen storage. *J. Mater. Sci. : Mater. Electron.,* 31(20): 17332-17338.

Muhammad, F.R., Jatranti, S., Qadariyah, L., dan Mahfud. 2014. Pembuatan biodiesel dari minyak nyamplung menggunakan pemanasan gelombang mikro. *Jurnal Teknik ITS,* 3(2): 154-159.

Nan, L., Yang, C., Jin, L., Wei, G., dan Wei, Z.Z., 2016. Preparation of Ni_2P/Zr-MCM-41 catalyst and its performance in the hydrodeoxygenation of *Jatropha curcas* oil. *J. Fuel Chem. Technol.,* 44(1): 76-83.

Nascimento, A.R.d., Alves, J.A.B.L.R., Melo, M.A.d.F., Melo, D.M.d.A., Souza, M.J.B.d., dan Pedrosa, A.M.G., 2015. Effect of the acid treatment of montmorillonite clay in the oleic acid esterification reaction. *Mater. Res.,* 18(2): 283-287.

Nasreen, S., Nafees, M., Qureshi, L.A., Asad, M.S., Sadiq, A., dan Ali, S.D. 2018. Review of Catalytic Transesterification Methods for Biodiesel Production. *In* Biofuels - State of Development. K. Biernat, ed. Pp. 93-119: Łukasiewicz R&D Network - Automotive Industry Institute.

Nguyen, H.K.D., dan Nguyen, D.T., 2017. Preparation of meso-structured silica–calcium mixed oxide (MSCMO) catalyst for converting Vietnamese rubber seed oil to biodiesel. *J. Porous Mater.,* 24(2): 443-454.

Nguyen, K.Q.N., Yen, N.T., Hau, N.D., dan Tran, H.L., 2020a. Synthesis and characterization of mesoporous silica SBA-15 and ZnO/SBA-15 photocatalytic materials from the ash of brickyards. *J. Chem.,* 2020: 1-8.

Ningsih, E., Suparto, Sato, A., Mustikasari, Y.R., dan Dewi, R.C., 2017. Ratio molar minyak sawit dengan etanol konsentrasi rendah dalam pembuatan biodiesel. *J.Tek. Kim.,* 12(1): 1-3.

Nomanbhay, S., dan Ong, M.Y., 2017. A Review of microwave-assisted reactions for biodiesel production. *Bioengineering (Basel, Switzerland),* 4(2): 1-21.

Norhasyimi, R., Ahmad Zuhairi, A., dan Abdullah Rahman, M., 2010. A review: mesoporous Santa Barbara Amorphous-15, types, synthesis and its applications towards biorefinery production. *Am. J. Appl. Sci.,* 7(12). 1579-1586.

Norsamsi, Fatonah, S., dan Iriani, D., 2015. Kemampuan tumbuh anakan tumbuhan nyamplung (*Calophyllum inophylum* L.) pada berbagai taraf penggenangan. *Biospecies,* 8(1): 20-28.

Nuntang, S., Yokoi, T., Tatsumi, T., dan Ngamcharussrivichai, C., 2016. Enhanced esterification of carboxylic acids with ethanol using propylsulfonic acid-functionalized natural rubber/hexagonal mesoporous silica nanocomposites. *Catal. Commun.,* 80: 5-9.

Nurhidayanti, N., 2018. Studi kinetika reaksi pembuatan biodiesel dari minyak nyamplung menggunakan iradiasi microwave. *Jurnal Tekno Insentif,* 12(2): 1-12.

Nuryono, and Narsito. 2005. Effect of acid concentration on characters of silica gel synthesized from sodium silicate. *Indones. J. Chem.,* 5(1): 23-30.

Obadiah, A., Swaroopa, G.A., Kumar, S.V., Jeganathan, K.R., dan Ramasubbu, A., 2012. Biodiesel production from palm oil using calcined waste animal bone as catalyst. *Bioresour. Technol.,* 116: 512-516.

Ong, H.C., Masjuki, H.H., Mahlia, T.M.I., Silitonga, A.S., Chong, W.T., dan Leong, K.Y., 2014. Optimization of biodiesel production and engine performance from high free fatty acid *Calophyllum inophylum* oil in CI diesel engine. *Energy Convers. Manag.,* 81: 30-40.

Onukwuli, D.O., Emembolu, L.N., Ude, C.N., Aliozo, S.O., dan Menkiti, M.C., 2017. Optimization of biodiesel production from refined cotton seed oil and its characterization. *Egypt. J. Pet.,* 26(1): 103-110.

Pachamuthu, M.P., Srinivasan, V.V., Karvembu, R., dan Luque, R., 2019. Preparation of mesoporous stannosilicates SnTUD-1 and catalytic activity in levulinic acid esterification. *Microporous Mesoporous Mater.,* 287: 159-166.

Pan, H., Li, H., Zhang, H., Wang, A., dan Yang, S., 2019. Acidic ionic liquid-functionalized mesoporous melamine-formaldehyde polymer as heterogeneous catalyst for biodiesel production. *Fuel,* 239: 886-895.

Pandian, S., Sakthi Saravanan, A., Sivanandi, P., Santra, M., dan Booramurthy, V.K. 2020. 4 - Application of heterogeneous acid catalyst derived from biomass for biodiesel process intensification: a comprehensive review. In refining biomass residues for sustainable energy and bioproducts. R.P. Kumar, E. Gnansounou, J.K. Raman, and G. Baskar, eds. Pp. 87-109: Academic Press.

Papirer, E. 2000. Adsorption on Silica Surfaces (1st ed.). CRC Press.

Patel, A., dan Pithadia, D., 2020. Low temperature synthesis of bio-fuel additives via valorisation of glycerol with benzaldehyde as well as furfural over a novel sustainable catalyst, 12-tungstosilicic acid anchored to ordered cubic nano-porous MCM-48. *Appl. Catal. A: Gen.,* 602: 117729.

Peiter, A.S., Lins, P.V.S., Meili, L., Soletti, J.I., Carvalho, S.H.V., Pimentel, W.R.O., dan Meneghetti, S.M.P., 2018. Stirring and mixing in ethylic biodiesel production. *J. King Saud Univ. Sci.*, 32(1): 54-59.

Persulessy, C.H., 2020. Kota ambon dalam angka, Penyediaan Data untuk Perencanaan Pembangunan.

Petkova, B., Tcholakova, S., Chenkova, M., Golemanov, K., Denkov, N., Thorley, D., dan Stoyanov, S., 2020. Foamability of aqueous solutions: Role of surfactant type and concentration. *Adv. Colloid Interface Sci.,* 276: 102084.

Pirouzmand, M., Anakhatoon, M.M., dan Ghasemi, Z., 2018a. One-step biodiesel production from waste cooking oils over metal incorporated MCM-41; positive effect of template. *Fuel,* 216: 296-300.

Pirouzmand, M., Gharehbaba, A.M., Ghasemi, Z., and Azizi Khaaje, S., 2017. [CTA]Fe/MCM-41: An efficient and reusable catalyst for green synthesis of xanthene derivatives. *Arab J. Chem.,* 10(8): 1070-1076.

Pirouzmand, M., Nikzad-kojanag, B., dan Seyed-Rasulzade, S.K., 2015. Surfactant containing Ca/MCM-41 as a highly active, green and reusable catalyst for the transesterification of canola oil. *Catal. Commun.,* 69: 196-201.

Pirouzmand, M., Seyed-Rasulzade, S.K., dan Nikzad-Kojanag, B., 2018b. Effect of preparation methods and pluronic template on the catalytic activity of Ca/SBA-15. *Iran J. Chem. Chem. Eng.,* 37(2): 53-60.

Priya, R., Khurana, I., dan Pandey, O.P., 2019. Synthesis of intense red light-emitting β-Ca_2SiO_4:Eu^{3+} phosphors for near UV-excited light-emitting diodes utilizing agro-food waste materials. *J. Mater. Sci.: Mater. Electron.,* 31(3): 1912-1928.

Priyanto, A., 2013. Eksplorasi nyamplung (*Calophyllum inophylum* L.) di sebaran alam Kalimantan Barat (Ketapang) untuk program pemuliaan pohon. *Informasi Teknis* 11(2): 69-78.

Pugazhenthi, G., Pakshirajan, K., Vinoth Kumar, R., dan Basumatary, A.K., 2017. Removal of trivalent metal ions from aqueous solution via crossflow ultrafiltration system using zeolite membranes. *J. Water Reuse Desal.,* 7(1): 66-76.

Purwanto, I., and Santosa, E., 2016. Hubungan mutu buah dan curah hujan terhadap kandungan asam lemak bebas pada minyak kelapa sawit. *Buletin Agrohorti,* 4: 250-255.

Putra, M.D., Irawan, C., Udiantoro, Ristianingsih, Y., dan Nata, I.F., 2018. A cleaner process for biodiesel production from waste cooking oil using waste materials as a heterogeneous catalyst and its kinetic study. *J. Clean. Prod.,* 195: 1249-1258.

Putranti, A.M.L.T., Wirawan, S.K., and Bendiyasa, I.M. 2018. Adsorption of free fatty acid (FFA) in low-grade cooking oil used activated natural zeolite as adsorbent. IOP Conference Series: Materials Science and Engineering, 2018. Vol. 299, pp. 012085. IOP Publishing.

Qian, X., Yang, J., Fei, Z., Liu, Q., Zhang, Z., Chen, X., Tang, J., Cui, M., and Qiao, X., 2019. A simple strategy to improve PEI dispersion on MCM-48 with long-alkyl chains template for efficient CO_2 adsorption. *Ind. Eng. Chem. Res.,* 58(25): 10975-10983.

Qiu, S., Zhou, H., Shen, Z., Hao, L., Chen, H., dan Zhou, X., 2020. Synthesis, characterization, and comparison of antibacterial effects and elucidating the mechanism of ZnO, CuO and CuZnO nanoparticles supported on mesoporous silica SBA-3. *RSC Adv.,* 10(5): 2767-2785.

Rajabi, F., dan Luque, R., 2014. An efficient renewable-derived surfactant for aqueous esterification reactions. *RSC Adv.,* 4(10): 5152–5155.

Rajabi, F., dan Luque, R., 2020. Highly ordered mesoporous functionalized pyridinium protic ionic liquids framework as efficient system in esterification reactions for biofuels production. *Mol. Catal.,* 498: 111238.

Ramli, N.A.S., Sivasubramaniam, D., dan Amin, N.A.S., 2017. Esterification of levulinic acid using ZrO_2-supported phosphotungstic acid catalyst for ethyl levulinate production. *Bioenergy Res.,* 10(4): 1105-1116.

Raqeeb, M.A., dan Bhargavi, R., 2015. Biodiesel Production from Waste Cooking Oil. *J. Chem. Pharm. Res.,* 7(12): 670-681.

Reddy, A.N.R., Saleh, A.A., Islam, M.S., Hamdan, S., Rahman, M.R., dan Masjuki, H.H., 2018. Experimental evaluation of fatty acid composition influence on Jatropha biodiesel physicochemical properties. *J. Renew. Sustain. Energy,* 10(1): 013103.

Ridhawati, Wahab, A.W., Nafie, N.L., dan Raya, I., 2018. Pengaruh metode sintesis silika mesopori SBA-15 terhadap analisis differential scanning calorimetry dan pengukuran low angles X-ray diffraction. *J. INTEK,* 5(1): 39-43.

Roev, V., Ma, S.B., Lee, D.J., dan Im, D., 2014. Lyophobized ordered mesoporous silica additives for Li-O_2 battery cathode. *J. Electrochem. Sci. Technol.,* 5(2): 58-64.

Roschat, W., Siritanon, T., Yoosuk, B., Sudyoadsuk, T., dan Promarak, V., 2017. Rubber seed oil as potential non-edible feedstock for biodiesel production using heterogeneous catalyst in Thailand. *Renew. Energy,* 101: 937-944.

Roth, W.J., 2009. Facile synthesis of the cubic mesoporous material MCM-48. Detailed study of accompanying phase transformations. *Adsorption,* 15(3): 221-226.

Sahu, G., Gupta, N.K., Kotha, A., Saha, S., Datta, S., Chavan, P., Kumari, N., dan Dutta, P., 2018. A review on biodiesel production through heterogeneous catalysis route. *Chem. Bio. Eng. Rev.,* 5(4): 231-252.

Sahu, G., Saha, S., Datta, S., Chavan, P., dan Naik, S., 2017. Methanolysis of Jatropha curcas oil using K_2CO_3/CaO as a solid base catalyst. *Turk. J. Chem.,* 41: 845-861.

Sahu, P., dan Sakthivel, A., 2021. Zeolite-β based molecular sieves: A potential catalyst for esterification of biomass derived model compound levulinic acid. *Mater. Sci. Energy Technol.,* 4: 307-316.

Said, N.H., Ani, F.N., dan Said, M.F.M., 2015. Review of the production of biodiesel from waste cooking oil using solid catalysts. *J. Mech. Eng. Sci.,* 8: 1302-1311.

Sajjadi, B., Raman, A.A.A., dan Arandiyan, H., 2016. A comprehensive review on properties of edible and non-edible vegetable oil-based biodiesel: Composition, specifications and prediction models. *Renew. Sustain. Energy Rev.,* 63: 62-92.

Salimi, Z., dan Hosseini, S.A., 2019. Study and optimization of conditions of biodiesel production from edible oils using ZnO/$BiFeO_3$ nano magnetic catalyst. *Fuel,* 239: 1204-1212.

Sam. 2020. Ciri ciri pohon bintangur (*Calophyllum inophylum*) di alam liar. https: // www. ciriciripohon. com / 2020 / 04 / ciri - ciri - pohon- bintangu r- di- alam-liar.html. 27-06-2020.

Samiey, B., Cheng, C.H., dan Wu, J., 2014. Organic-inorganic hybrid polymers as adsorbents for removal of heavy metal ions from solutions: A review. *Mater.,* 7: 673-726.

Samik. 2011. Aktivitas katalis K_3PO_4/NaZSM-5 mesopori pada transesterifikasi refined palm oil (RPO) menjadi biodiesel, Tesis belum dipublikasi. Surabaya : Program Pascasarjana Kimia. Fakultas Matematika dan Ilmu Pengetahuan Alam. Institut Teknologi Sepuluh Nopember.

Sanday, T.A. 2011. Analisa teknoekonomi pendirian industri biodiesel dari biji nyamplung (*Calophyllum inophylum* L.). Skripsi belum dipublikasi, Bogor : Program Sarjana Teknologi Pertanian. Institut Pertanian Bogor.

Sani, Y.M., Dauda, W.M.A.W., dan Aziz, A.R.A., 2014. Activity of solid acid catalysts for biodiesel production: A critical review. *Appl. Catal. A : Gen.,* 470 140-161.

Sanjid, A., Masjuki, H.H., Kalam, M.A., Rahman, S.M.A., Abedin, M.J., dan Palash, S.M., 2013. Impact of palm, mustard, waste cooking oil and *Calophyllum inophylum* biofuels on performance and emission of CI engine. *Renew. Sustain. Energy Rev.,* 27: 664-682.

Sannino, M., Del Piano, L., Abet, M., Baiano, S., Crimaldi, M., Modestia, F., Raimo, F., Ricciardiello, G., dan Faugno, S., 2017. Effect of mechanical extraction parameters on the yield and quality of tobacco (*Nicotiana tabacum* L.) seed oil. *J. Food Sci. Technol.,* 54(12): 4009-4015.

Santoso, H., Kristianto, I., dan Setyadi, A. 2013. Pembuatan biodiesel menggunakan katalis basa heterogen berbahan dasar kulit telur, Lembaga Penelitian dan Pengabdian kepada Masyarakat, Universitas Katolik Prahayangan.

Saravanan, K., Tyagi, B., dan Bajaj, H.C., 2016. Nano-crystalline, mesoporous aerogel sulfated zirconia as an efficient catalyst for esterification of stearic acid with methanol. *Appl. Catal. B: Environ.,* 192: 161-170.

Sari, A.Y.P., Taba, P., and Budi, P., 2015. Synthesis and characterization of the MCM-48 and modified NH_2. *Indo. J. Chem. Res.,* 3: 249-253.

SathyaSelvabala, V., Selvaraj, D.K., Kalimuthu, J., Periyaraman, P.M., dan Subramanian, S., 2011. Two-step biodiesel production from *Calophyllum inophylum* oil: optimization of modified beta-zeolite catalyzed pre-treatment. *Bioresour. Technol.,* 102(2): 1066-1072.

Sazegar, M.R., Dadvand, A., dan Mahmoudi, A., 2017. Novel protonated Fe-containing mesoporous silica nanoparticle catalyst: excellent performance cyclohexane oxidation. *RSC Adv.,* 7(44): 27506-27514.

Seffati, K., Esmaeili, H., Honarvar, B., dan Esfandiari, N., 2020. AC/$CuFe_2$O4@CaO as a novel nanocatalyst to produce biodiesel from chicken fat. *Renew. Energy,* 147: 25-34.

Semwal, S., Arora, A.K., Badoni, R.P., dan Tuli, D.K., 2011. Biodiesel production using heterogeneous catalysts. *Bioresour. Technol.,* 102(3): 2151-2161.

Seo, J.W., Lee, W.-J., Nam, S., Ryoo, H., Kim, J.-N., dan Ko, C.H., 2015. Mesoporous Structure Control of Silica in Room-Temperature Synthesis under Basic Conditions. *J. Nanomater.,* 2015: 1-7.

Serio, M.D., Tesser, R., Pengmei, L., dan Santacesaria, E., 2008. Heterogeneous catalysts for biodiesel production. *Energy Fuels,* 22: 207-217.

Setiadi 2011 Reaksi konversi katalitik aseton menjadi hidrokarbon aromatik menggunakan katalis H-ZSM-5. Disertasi belum dipublikasi, Teknik Kimia Universitas Indonesia. Depok.

Shagufta, Ahmad, I., dan Dhar, R., 2017. Sulfonic acid-functionalized solid acid catalyst in esterification and transesterification reactions. *Catal Surv. Asia,* 21(2): 53-69.

Sharma, S., Saxena, V., Baranwal, A., Chandra, P., dan Pandey, L.M., 2018. Engineered nanoporous materials mediated heterogeneous catalysts and their implications in biodiesel production. *Mater. Sci. Energy Technol.,* 1(1): 11-21.

Singh, D., Sharma, D., Soni, S.L., Sharma, S., Kumar Sharma, P., dan Jhalani, A., 2020. A review on feedstocks, production processes, and yield for different generations of biodiesel. *Fuel,* 262: 116553.

Singh, S., dan Patel, A., 2014. 12-Tungstophosphoric acid supported on mesoporous molecular material: synthesis, characterization and performance in biodiesel production. *J. Clean. Prod.,* 72: 46-56.

Siow, H.S., Sudesh, K., Murugan, P., dan Ganesan, S., 2021. Mealworm (*Tenebrio molitor*) oil characterization and optimization of the free fatty acid pretreatment via acid-catalyzed esterification. *Fuel,* 299.

Slamet, S., dan Dewi, A.S.C., 2018. Synthesis of biodiesel from waste cooking oil using heterogeneous CaO catalyst: Effect of stirring speed. *AIP Conference Proceedings,* 2024(1): 020060.

Solis, J.L., Alejo, L., dan Kiros, Y., 2016. Calcium and tin oxides for heterogeneous transesterification of babasssu oil (*Attalea speciosa*). *J. Environ. Chem. Eng.,* 4(4, Part B): 4870-4877.

Song, R., Tong, D., Tang, J., dan Hu, C., 2011. Effect of composition on the structure and catalytic properties of KF/Mg–La solid base catalysts for biodiesel synthesis via transesterification of cottonseed oil. *Energy Fuels,* 25(6): 2679-2686.

Suleman, N., Abas, dan Paputungan, M., 2019. Esterifikasi dan transesterifikasi stearin sawit untuk pembuatan biodiesel. *J. Tek.,* 17(1): 66-77.

Sunarno, Bahri, S., and Utama, P.S., 2011. Catalytic slurry cracking cangkang sawit menjadi crude bio-fuel dengan katalis Ni/ZSM-5 dan NiMo/ZSM-5. Hibah Bersaing, Universitas Riau.

Sundaryono, A., 2010. Karakteristik Biodiesel dan Blending Biodiesel dari Oil Losses Limbah Cair Pabrik Minyak Kelapa Sawit. *J. Tek. Ind. Pert.,* 21(1): 34-40.

Susila, I.W.W. 2018. Nyamplung tanaman multifungsi potensi sebaran dan manfaatnya di Nusa Tenggara Barat dan Bali: PT kanisius (Anggota IKAPI).

Sutapa, I.W. 2019. Sintesis, modifikasi nano katalis mgo pada montmorilonit untuk aplikasi produksi biodiesel dari minyak *Cerbera odollam,* Disertasi belum dipublikasi, Departemen Kimia, Universitas Hasanuddin.

Syamsidar, H.S., 2013. Pembuatan dan uji kualitas biodiesel dari minyak jelantah. *J. Teknosains,* 7: 209-218.

Syarifudin, Suprihadi, A., Nurcahyo, H., dan Dairoh. 2019. Pengaruh viskositas biodiesel campuran solar-minyak sawit-alkohol terhadap potensi penurunan performa dan peningkatan emisi jelaga. Prosiding SNATIF, Universitas Muria Kudus, 2019. Vol. 6. SNATIF.

Taba, P., 2008. Adsorption of water and benzene vapour in mesoporous materials. *Makara J. Sci.,* 12(2): 120-125.

Taba, P., Budi, P., Gau, A., Hala, Y., Fauziah, S., Sutapa, I.W., dan Manga, J., 2021a. Mesoporous silica modified with amino group (NH_2-MCM-48) as adsorbent of Ag(I) and Cr(III) in water. *Rasayan J. Chem.,* 14: 204-211.

Taba, P., Budi, P., dan Puspitasari, A.Y. 2017. Adsorption of heavy metals on amine-functionalized MCM-48. IOP Conference Series: Materials Science and Engineering, 188, pp. 012015. IOP Publishing.

Taba, P., Jannah, M., dan Hala, Y., 2021b. Mesoporous silica MCM-48 as chloramphenicol adsorbent. *Indones. J. Chem. Res.,* 8: 242-246.

Taba, P., Natsir, H., Fauziah, S., dan Ismail, M., 2010. Adsorpsi ion Cd(II) oleh kitosan-silika mesopori MCM-48. *Mar. Chim. Acta.,* 11(1): 13-22.

Tanglumlert, W., Imae, T., White, T.J., dan Wongkasemjit, S., 2009. Styrene oxidation with H_2O_2 over Fe- and Ti-SBA-1 mesoporous silica. *Catal. Commun.,* 10(7): 1070-1073.

Trisunaryanti, W., Triyono, Paramesti, C., Larasati, S., Santoso, N.R., dan Fatmawati, D.A. 2020. Synthesis and characterization of Ni-NH_2/mesoporous silica catalyst from lapindo mud for hydrocracking of waste cooking oil into biofuel. *Rasayan J. Chem*., 13(3): 1386-1393.

Turkkul, B., Deliismail, O., dan Seker, E., 2020. Ethyl esters biodiesel production from *Spirulina* sp. and *Nannochloropsis oculata* microalgal lipids over alumina-calcium oxide catalyst. *Renew. Energy,* 145: 1014-1019.

Utomo, M.P., and Laksono, E.W. 2007. Tinjauan umum tentang deaktivasi katalis pada reaksi katalisis heterogen. Prosiding Seminar Nasional Penelitian, Pendidikan dan Penerapan MIPA, Yogyakarta, 2007. Universitas Negeri Yogyakarta.

Vifttaria, M., Nurhayati, dan Anita, S. 2019. Surface acidity of sulfuric acid activated maredan clay catalysts with boehm titration method and pyridine adsorption-FTIR. J. Phys. : Conf. Ser., 1351. IOP Publishing.

Vogel, A.I., Tatchell, A.R., Furnis, B.S., Hannaford, A.J., and Smith, P.W.G. 1996. Vogel's Textbook of Practical Organic Chemistry: New York. John Wiley & Sons.

Vrålstad, T., Øye, G., Stöcker, M., dan Sjöblom, J., 2007. Synthesis of comparable Co-MCM-48 and Co-MCM-41 materials containing high cobalt contents. *Microporous Mesoporous Mater.,* 104: 10-17.

Wan, H., Wu, Z., Chen, W., Guan, G., Cai, Y., Chen, C., Li, Z., dan Liu, X., 2015. Heterogenization of ionic liquid based on mesoporous material as magnetically recyclable catalyst for biodiesel production. *J. Mol. Catal. A: Chem.,* 398: 127-132.

Wang, J., Wang, G., Zhang, Z., Ouyang, G., dan Hao, Z., 2021. Effects of mesoporous silica particle size and pore structure on the performance of polymer-mesoporous silica mixed matrix membranes. *RSC Adv.,* 11(58): 36577-36586.

Wang, Y.-T., Fang, Z., Yang, X.-X., Yang, Y.-T., Luo, J., Xu, K., dan Bao, G.-R., 2018. One-step production of biodiesel from Jatropha oils with high acid value at low temperature by magnetic acid-base amphoteric nanoparticles. *Chem. Eng. J.,* 348: 929-939.

Wang, Y.-Y., dan Chen, B.-H., 2016. High-silica zeolite beta as a heterogeneous catalyst in transesterification of triolein for biodiesel production. *Catal. Today,* 278(Part 2): 335-343.

Wen, H., Zhou, X., Shen, Z., Peng, Z., Chen, H., Hao, L., dan Zhou, H., 2019. Synthesis of ZnO nanoparticles supported on mesoporous SBA-15 with coordination effect - assist for anti-bacterial assessment. *Colloids Surf. B: Biointerfaces,* 181: 285-294.

Wibowo, A.E., Saputra, A.K., and Susidarti, R.A., 2018. Optimasi sintesis senyawa 1-(2,5-dihidroksifenil)-(3-piridin-2-il) propenon sebagai antiinflamasi menggunakan variasi katalis NaOH. *Pharmaceutical J. Indones.,* 15(2): 202-208.

Widiarti, N., Lailun Ni'mah, Y., Bahruji, H., dan Prasetyoko, D., 2019. Development of CaO from natural calcite as a heterogeneous base catalyst in the formation of biodiesel: Review. *J. Renew. Mater.,* 7(10): 915-939.

Wilkanowicz, S.I., Hollingsworth, N.R., Saud, K., Kadiyala, U., dan Larson, R.G., 2020. Immobilization of calcium oxide onto polyacrylonitrile (PAN) fibers as a heterogeneous catalyst for biodiesel production. *Fuel Process. Technol.,* 197: 106214.

Wong, Y.C., dan Ang, R.X., 2018. Study of calcined eggshell as potential catalyst for biodiesel formation using used cooking oil. *Open Chem.,* 16(1): 1166-1175.

Wu, J., Mei, P., Wu, J., Fu, J.-W., Cheng, L., dan Lai, L., 2020. Surface properties and microemulsion of anionic/nonionic mixtures based on sulfonate Gemini surfactant in the presence of NaCl. *J. Mol. Liq.,* 317: 113907.

Xia, Q.H., Su, K.X., Ma, X.T., Ge, H.Q., and Zhu, H.B., 2005. Efficiently tailoring the pore diameter of mesoporous MCM-48 to micropore. *Materials Letters,* 59(17): 2110-2114.

Xia, Y., dan Mokaya, R., 2003. A study of the behaviour of mesoporous silicas in OH/CTABr/H_2O systems: phase dependent stabilisation, dissolution or semi-pseudomorphic transformation. *J. Mater. Chem.,* 13(12): 3112–3121.

Yin, Y., Zhao, H., Prabhakar, M., dan Rohwerder, M., 2022. Organic composite coatings containing mesoporous silica particles: Degradation of the SiO_2 leading to self-healing of the delaminated interface. *Corrosi. Sci.,* 200: 110252.

Yuliana, Veronica, J.S., Indraswati, N., dan Gunantara, B., 2005. Penggunaan adsorben untuk mengurangi kadar free fatty acid, peroxide value dan warna minyak goreng bekas. *J. Tek. Kim. Indones.,* 4(2): 212-218.

Yusuf, A., 2018. A review of methods used for seed oil extraction. *Int. J. Sci. Res.,* 7: 233-238.

Yusuff, A.S., Adeniyi, O.D., Olutoye, M.A., dan Akpan, U.G., 2018. Development and characterization of a composite anthill-chicken eggshell catalyst for biodiesel production from waste frying oil. *Int. J. . Technol.,* 9(1): 110-119.

Zanelato, C.B., Pires, A.F., da Silva, S.N., dan Galdino, A.G.S., 2020. Development of biphasic bone cement obtained from chicken eggshell. *J. Mater. Res. Technol.,* 9(4): 7297-7304.

Zappaterra, F., Rodriguez, M.E.M., Summa, D., Semeraro, B., Costa, S., dan Tamburini, E., 2021. Biocatalytic Approach for Direct Esterification of Ibuprofen with Sorbitol in Biphasic Media. *Int. J. Mol. Sci.,* 22(6): 1-18.

Zhang, R., Zhu, F., Dong, Y., Wu, X., Sun, Y., Zhang, D., Zhang, T., dan Han, M., 2020b. Function promotion of $SO_4^{2-}/Al_2O_3–SnO_2$ catalyst for biodiesel production from sewage sludge. *Renew. Energy,* 147: 275-283.

Zhang, X., Ma, Q., Cheng, B., Wang, J., Li, J., dan Nie, F., 2012. Research on KOH/La-Ba-Al_2O_3catalysts for biodiesel production via transesterification from microalgae oil. *J. Nat. Gas Chem.,* 21: 774-779.

Zhao, Q., Mao, Y., Yan, L., Lu, L., Jiang, T., dan Yin, H., 2018. Stability of Y/MCM-48 composite molecular sieve with mesoporous and microporous structures. *J. Asian Ceram. Soc.,* 2(4): 347-356.

Zhuravlev, L.T., and Potapov, V.V., 2006. Density of silanol groups on the surface of silica precipitated from a hydrothermal solution. *Russ. J. Phys. Chem.,* 80(7): 1119-1128.

Zul, N.A., Ganesan, S., Hamidon, T.S., Oh, W.-D., dan Hussin, M.H., 2021. A review on the utilization of calcium oxide as a base catalyst in biodiesel production. *J. Environ. Chem. Eng.,* 9(4): 105741.

LAMPIRAN

Lampiran 1. Skema prosedur kerja

a. Penyiapan sampel

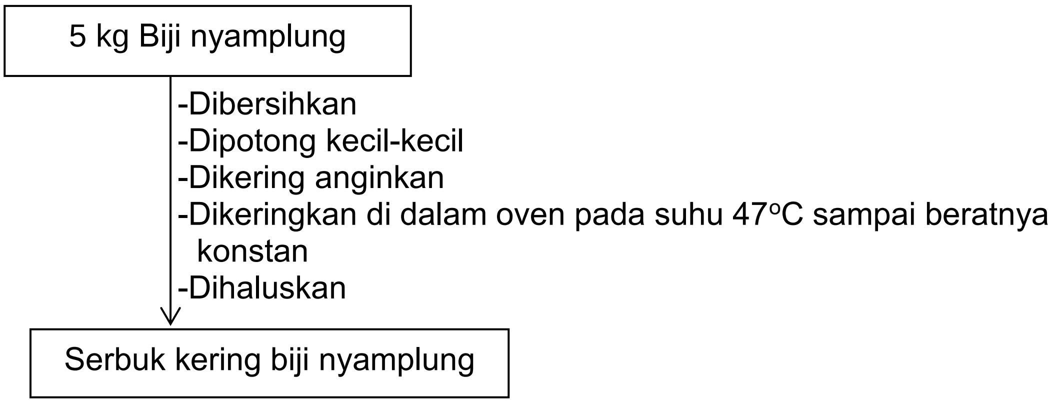

b. Ekstraksi minyak biji nyamplung

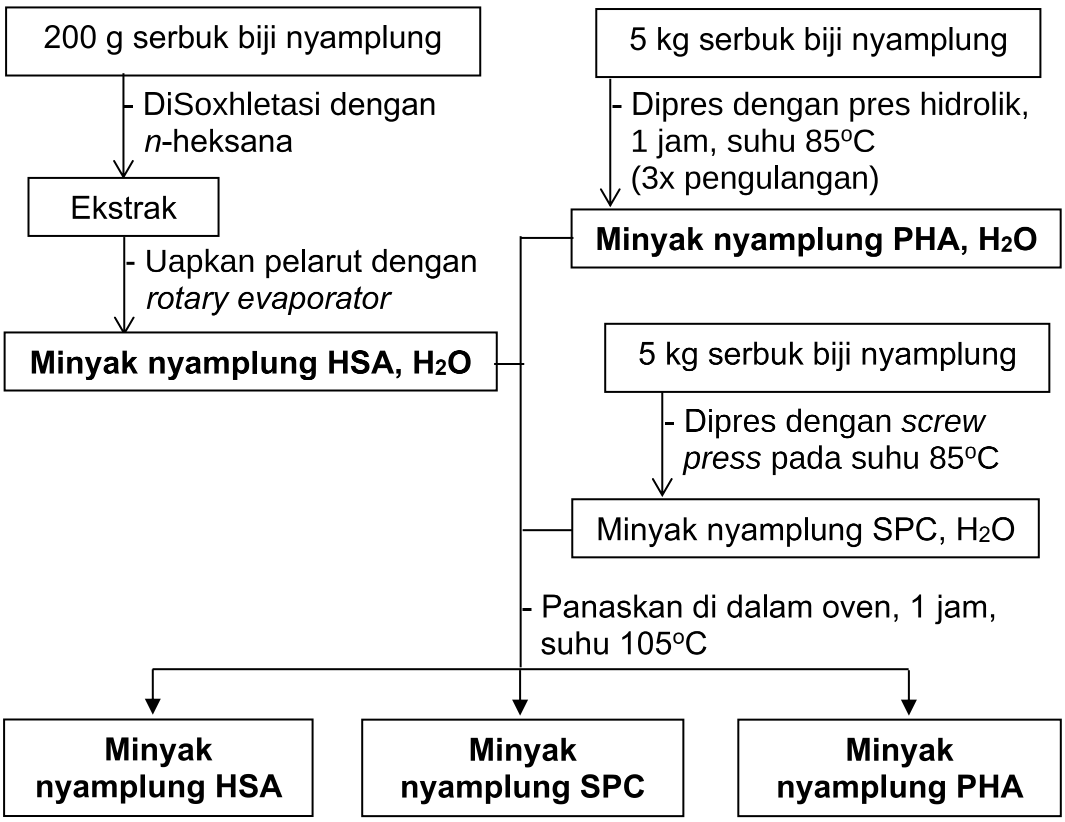

c. *Degumming*

Minyak nyamplung

- Dipanaskan pada suhu 65 ^oC
+ 5% (v/v) H_3PO_4 85%
- Diaduk dengan kecepatan 1000 rpm, 1 jam

↓

Campuran minyak, getah, dan H_3PO_4

- Didiamkan selama 12 jam
- Didekantasi

↓

Campuran minyak dan sisa H_3PO_4

- Dicuci dengan akuades (60-80 ^oC) hingga pH netral
- Didiamkan selama 12 jam pada suhu ruang
- Disaring dengan kertas saring melalui corong Buchner
- Panaskan di dalam oven, 1 jam, suhu 105^oC

↓

Minyak nyamplung murni

d. Sintesis katalis MCM-48

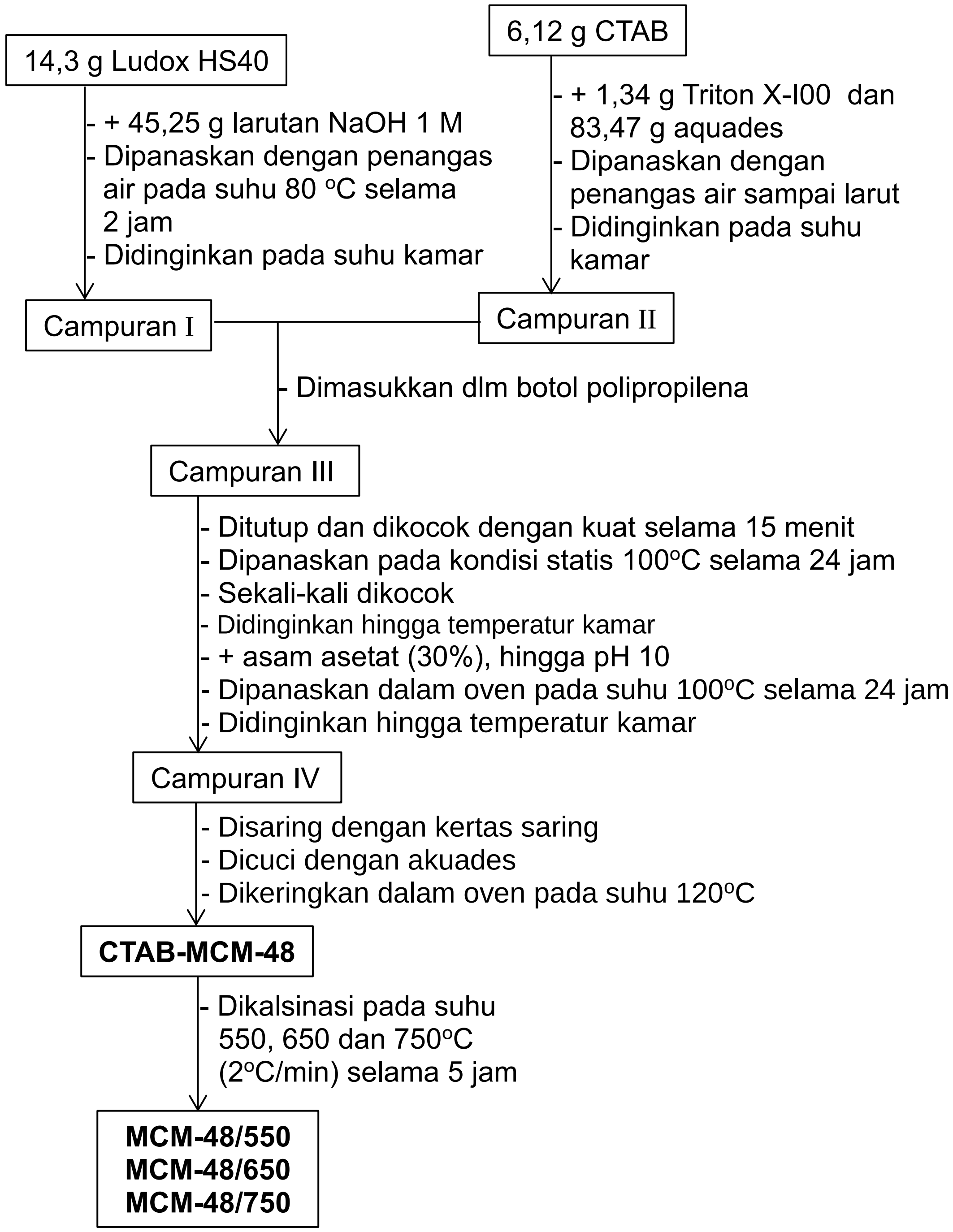

e. Sintesis katalis MCM-48/NaCl

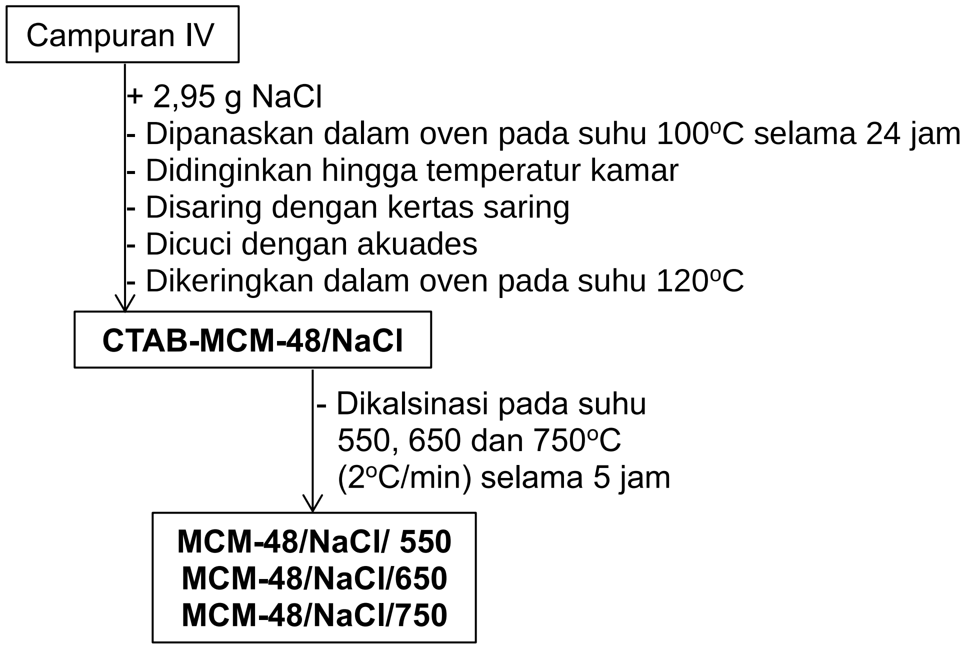

f. Sintesis katalis ZMC

1. Metode A

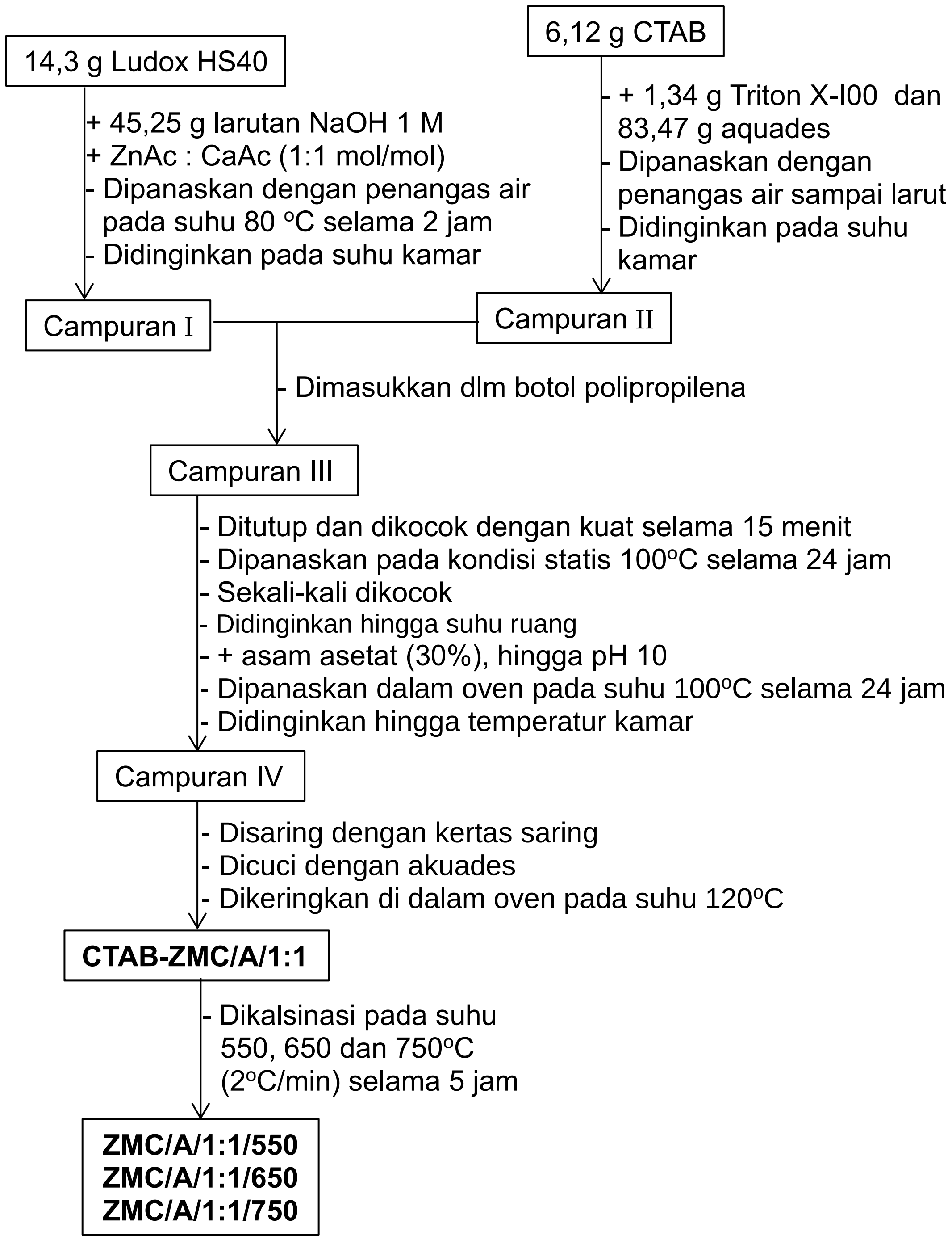

2. Metode B

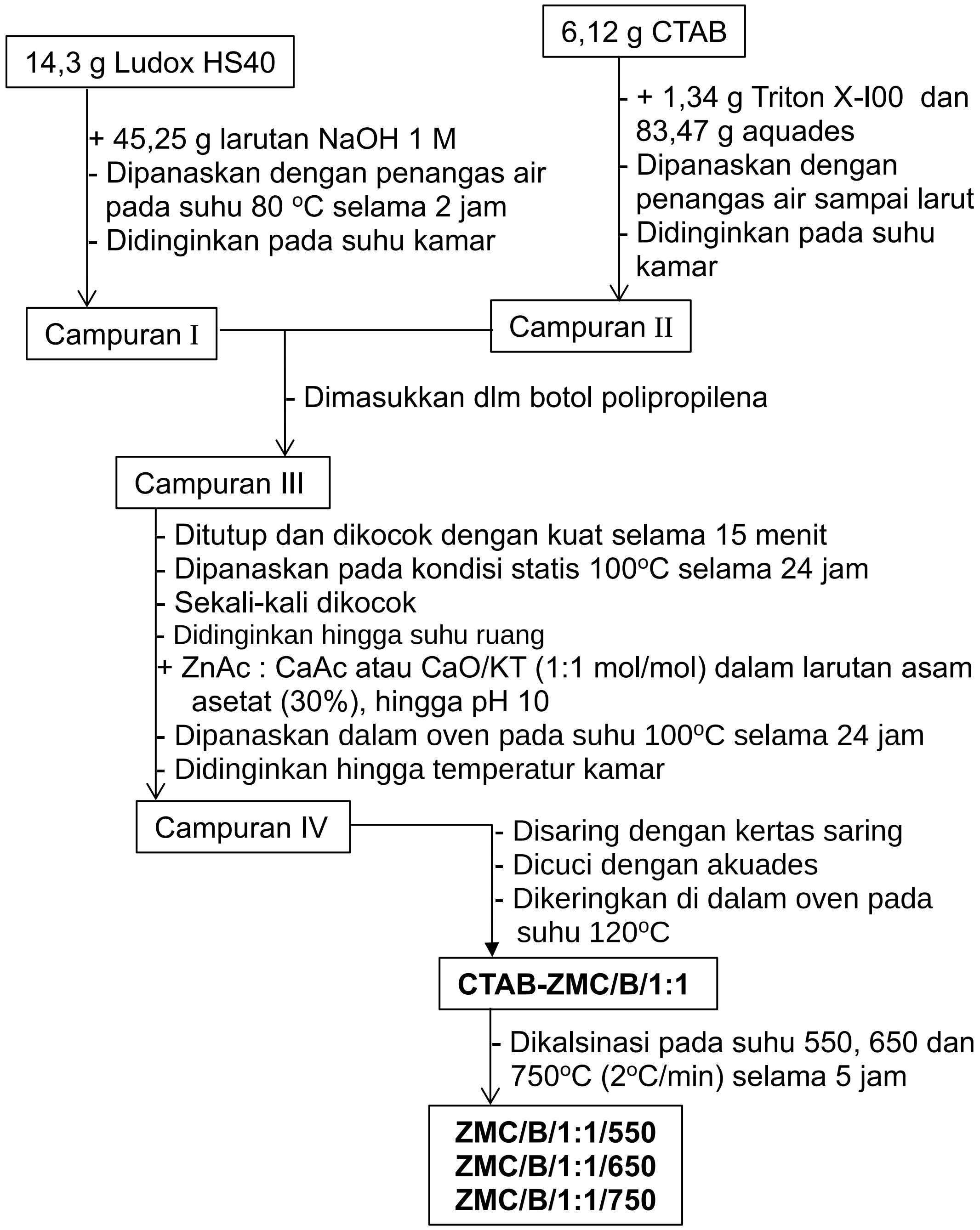

Catatan : 1) Metode B digunakan untuk sintesis katalis CTAB-ZMC/B/1: 0, CTAB-ZMC/B/1: 4, CTAB-ZMC/B/1: 8, CTAB-ZMC/B/1: 16 dan CTAB-ZMC/B/1: 32. 2) Semua katalis dikarakterisasi dengan XRD, FTIR, XRF, BET, SEM dan diuji aktivitasnya pada reaksi esterifikasi minyak nyamplung.

g. Penetuan keasaman katalis

10 mL Piridin

- Dimasukkan dalam cawan petri
- Ditempatkan dalam desikator, 24 Jam

Desikator yang jenuh dengan uap piridin

0,1 g Katalis

- Dimasukkan dalam cawan petri

Cawan + Uap piridin + Katalis

Ditempatkan dalam desiktor, 24 jam

Desikator yang jenuh dengan uap piridin

- Dibuka penutup desikator, 1 jam
- Ditimbang
- Hitung keasaman katalis

Data

h. Penentuan kadar FFA

2 gram minyak nyamplung

+ 20 mL metanol panas yang telah dinetralkan sebelumnya dengan NaOH
+ 3 tetes indikator PP

Larutan berwarna bening

- Dititrasi dengan NaOH hingga warna keunguan pada larutan dan tidak hilang sampai 15 detik

Larutan berwarna keunguan — Hitung kadar FFA

i. Esterifikasi minyak nyamplung

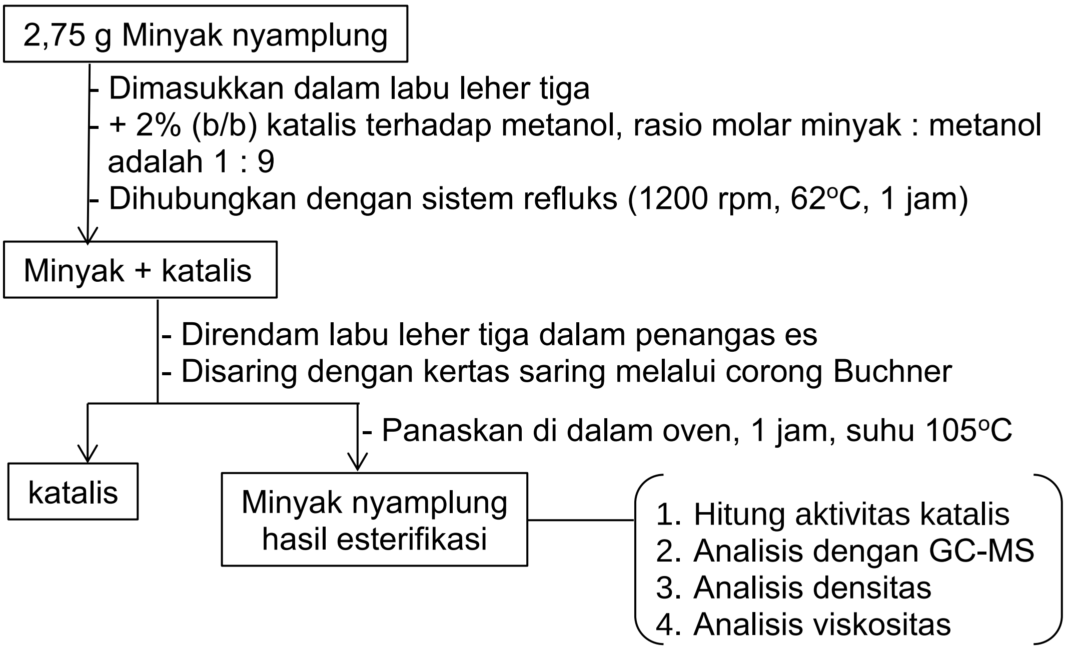

Catatan : Prosedur yang sama diterapkan untuk uji aktivitas katalis, optimasi komposisi kimia katalis ZMC, suhu (45, 50, 55, 60, 65 dan 80ºC), waktu (1, 2, 3, 4 dan 5 jam) jumlah metanol (metanol: minyak (b/b); 1: 0,5, 1: 1, 1: 2, 1: 3 dan 1: 6), jumlah katalis (katalis : metanol (b/b); 1: 4, 1: 6, 1: 8, 1: 16 dan 1: 27), laju pengadukan (120, 240, 480, 720, 960, 1200 dan 1440 rpm), penggunaan kembali katalis (pertama, kedua dan ketiga), sumber CaO (komersil dan kulit telur ayam) dan sumber minyak nyamplung (HSA, PHA dan SPC).

Lampiran 2. Kadar air biji nyamplung

✓ **Contoh perhitungan untuk minyak nyamplung HSA**

1. Berat sampel basah = 5 g
2. Berat sampel kering = 3,45 g

$$\text{Kadar air} = \frac{(\text{Berat sampel basah - berat sampel kering})}{\text{Berat sampel basah}} \times 100\%$$

$$\text{Kadar air} = \frac{(5\text{ g} - 3{,}45\text{ g})}{5\text{ g}} \times 100\%$$

$$\text{Kadar air} = \frac{(5\text{ g} - 3{,}45\text{ g})}{5\text{ g}} \times 100\%$$

Kadar air = 31%

Lampiran 3. Kadar minyak biji nyamplung

✓ **Contoh perhitungan untuk minyak nyamplung HSA**

1. Berat biji nyamplung = 156,28 g
2. Berat minyak nyamplung = 117,43 g

$$\text{Kadar minyak} = \frac{\text{Berat minyak nyamplung}}{\text{Berta biji nyamplung}} \times 100\%$$

$$\text{Kadar minyak} = \frac{117{,}43\text{ g}}{156{,}28\text{ g}} \times 100\%$$

Kadar minyak = 75,14%

Perhitungan sama untuk minyak nyamplung PUA dan SPC yang nilanya ditampilkan pada tabel berikut.

Lampiran 4. Spektrum FTIR katalis CTAB-MCM-48

SHIMADZU

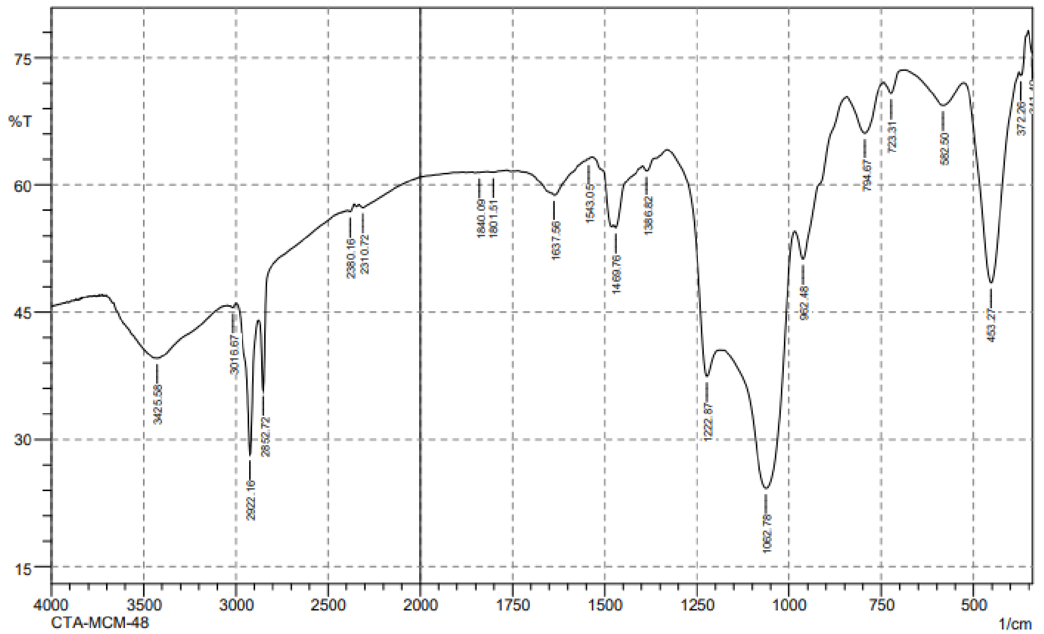

No.	Peak	Intensity	Corr. Intensity	Base (H)	Base (L)	Area	Corr. Area
1	341.4	75.598	0.482	351.04	339.47	1.359	0.024
2	372.26	72.906	1.166	376.12	352.97	2.844	0.086
3	453.27	48.469	24.166	526.57	378.05	31.745	11.135
4	582.5	69.381	3.155	686.66	528.5	23.211	1.368
5	723.31	70.767	1.828	742.59	688.59	7.63	0.209
6	794.67	66.087	5.117	842.89	744.52	16.06	1.567
7	962.48	51.272	5.676	983.7	844.82	30.267	1.762
8	1062.78	24.242	24.907	1186.22	985.62	92.001	26.384
9	1222.87	37.444	8.926	1328.95	1188.15	41.3	2.515
10	1386.82	61.673	0.835	1396.46	1330.88	13.176	0.118
11	1469.76	54.981	0.785	1475.54	1398.39	17.326	0.06
12	1543.05	63.019	0.093	1546.91	1535.34	2.311	0.002
13	1637.56	58.806	3.396	1712.79	1546.91	35.937	1.82
14	1801.51	61.499	0.062	1805.37	1788.01	3.658	0.005
15	1840.09	61.479	0.027	1843.95	1832.38	2.443	0.001
16	2310.72	57.342	0.561	2331.94	1980.89	79.767	0.413
17	2380.16	56.824	0.402	2391.73	2358.94	7.972	0.058
18	2852.72	35.803	8.856	2875.86	2393.66	134.664	1.522
19	2922.16	28.219	16.55	2999.31	2877.79	49.335	7.207
20	3016.67	45.536	0.317	3030.17	3001.24	9.841	0.05
21	3425.58	39.559	0.147	3433.29	3045.6	143.286	0.207

Comment;
CTA-MCM-48

Date/Time; 8/5/2020 9:44:46 AM
No. of Scans;
Resolution;
Apodization;

Lampiran 5. Spektrum FTIR katalis MCM-48/550

SHIMADZU

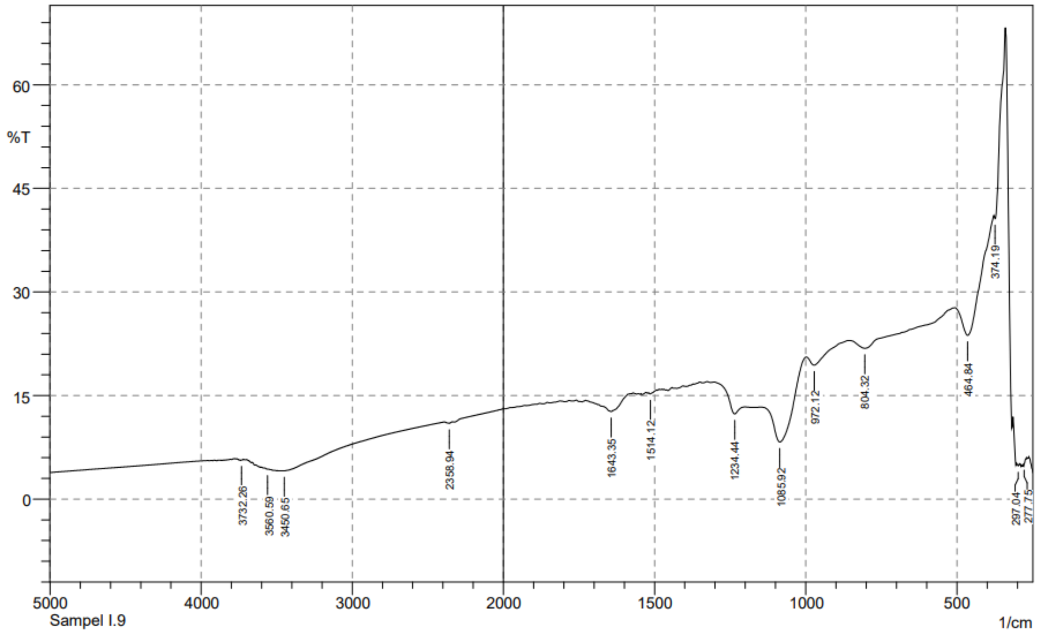

No.	Peak	Intensity	Corr. Intensity	Base (H)	Base (L)	Area	Corr. Area
1	248.82	3.821	0	262.32	248.82	17.486	-0.266
2	277.75	4.797	0.24	279.68	270.03	12.092	0
3	297.04	4.813	0.342	302.82	293.18	12.568	0.156
4	374.19	40.609	3.189	378.05	339.47	11.054	0.405
5	464.84	23.708	8.266	505.35	378.05	67.465	7.41
6	804.32	21.844	1.479	856.39	680.87	112.038	1.834
7	972.12	19.408	1.588	997.2	856.39	94.761	1.434
8	1085.92	8.274	8.021	1147.65	997.2	135.65	18.133
9	1234.44	12.346	2.164	1303.88	1201.65	85.668	1.583
10	1514.12	15.241	0.256	1519.91	1492.9	21.886	0.11
11	1643.35	12.677	0.31	1649.14	1581.63	58.059	0.362
12	2358.94	10.984	0.209	2391.73	2337.72	51.6	0.232
13	3450.65	4.096	0.041	3456.44	2391.73	1179.566	0.119
14	3560.59	4.343	0.047	3577.95	3554.81	31.424	0.077
15	3732.26	5.657	0.023	3734.19	3720.69	16.806	0.031

Comment;
Sampel I.9

Date/Time; 2/1/2021 11:54:39 AM
No. of Scans;
Resolution;
Apodization;

Lampiran 6. Spektrum FTIR katalis MCM-48/650

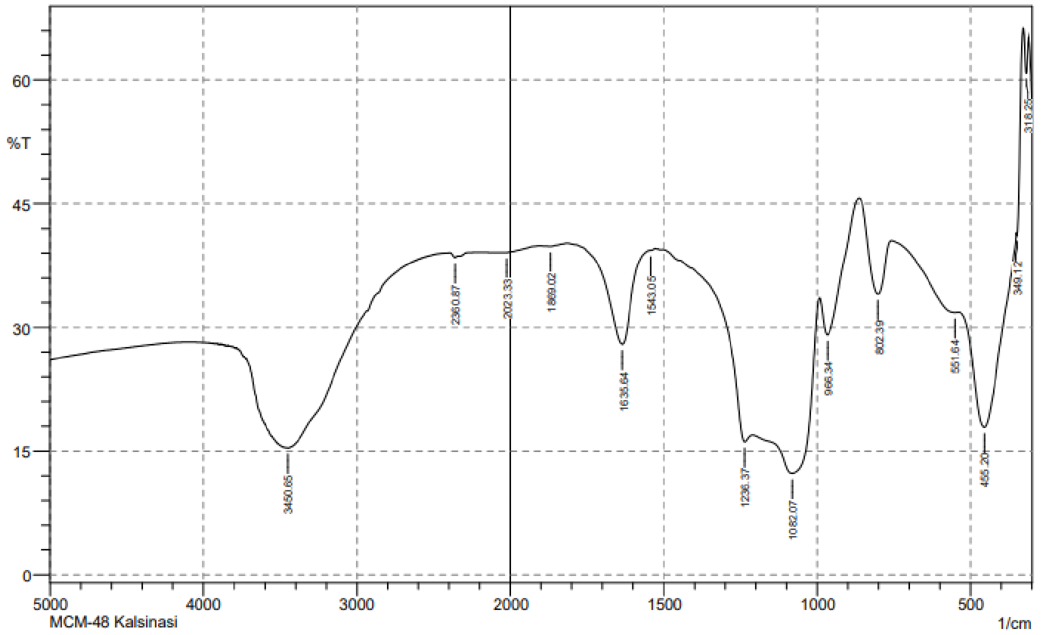

No.	Peak	Intensity	Corr. Intensity	Base (H)	Base (L)	Area	Corr. Area
1	318.25	60.851	4.752	327.9	310.54	3.487	0.308
2	349.12	41.191	2.441	351.04	329.83	5.866	0.258
3	455.2	17.865	18.19	538.14	351.04	108.522	26.256
4	551.64	31.795	0.487	758.02	540.07	96.767	0.753
5	802.39	34.038	8.605	862.18	759.95	42.574	5.061
6	966.34	29.078	6.853	991.41	864.11	56.675	5.031
7	1082.07	12.301	14.42	1209.37	993.34	171.225	36.962
8	1236.37	16.119	2.763	1500.62	1211.3	148.333	1.246
9	1543.05	39.326	0.039	1544.98	1529.55	6.239	0.006
10	1635.64	27.942	11.685	1813.09	1544.98	119.583	12.191
11	1869.02	39.799	0.102	1880.6	1815.02	26.114	0.031
12	2023.33	39.068	0.027	2027.19	1905.67	49.094	0.059
13	2360.87	38.469	0.306	2393.66	2343.51	20.684	0.081
14	2065.76	15.386	0.2	3458.37	2395.59	575.642	0.539

Comment;

MCM-48 Kalsinasi

Date/Time; 9/23/2020 1:17:07 PM

No. of Scans;

Resolution;

Apodization;

Lampiran 7. Spektrum FTIR katalis MCM-48/750

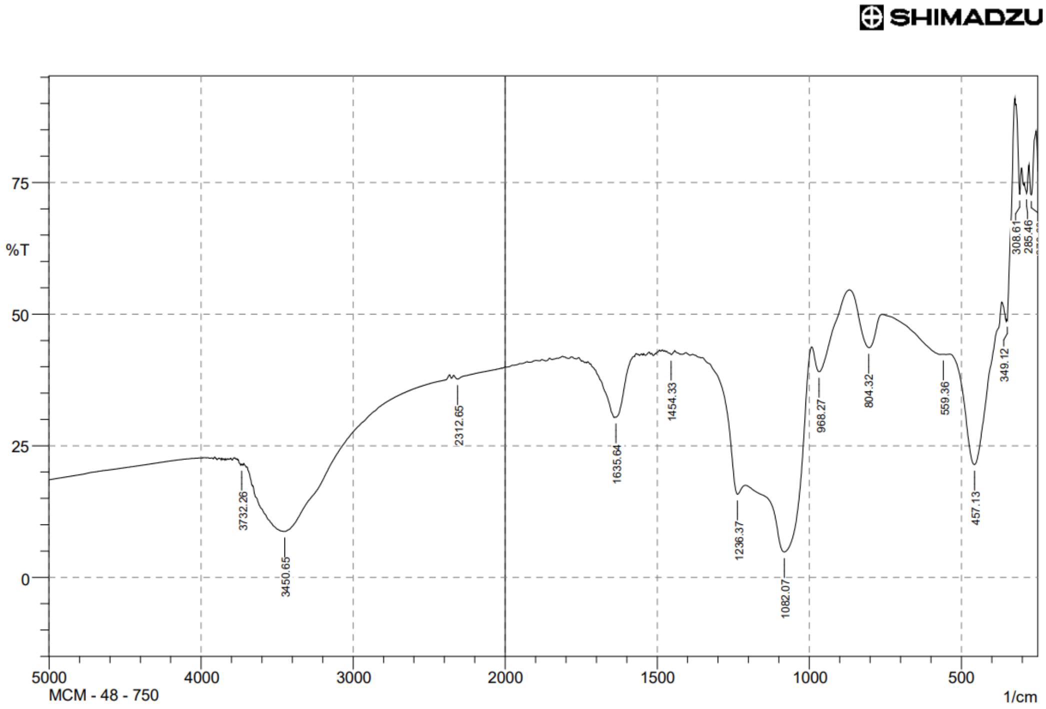

No.	Peak	Intensity	Corr. Intensity	Base (H)	Base (L)	Area	Corr. Area
1	248.82	77.09	0	254.6	248.82	0.5	-0.03
2	248.82	77.09	0	254.6	248.82	0.5	-0.03
3	248.82	77.09	0	254.6	248.82	0.5	-0.03
4	248.82	77.09	0	254.6	248.82	0.5	-0.03
5	248.82	77.09	0	254.6	248.82	0.5	-0.03
6	248.82	77.09	0	254.6	248.82	0.5	-0.03
7	248.82	77.09	0	254.6	248.82	0.5	-0.03
8	248.82	77.09	0	254.6	248.82	0.5	-0.03
9	248.82	77.09	0	254.6	248.82	0.5	-0.03
10	270.03	72.63	7.84	277.75	254.6	2.53	0.47
11	285.46	72.94	3.65	293.18	277.75	1.95	0.16
12	308.61	72.75	9.03	320.18	302.82	1.73	0.37
13	349.12	48.75	3.24	351.04	324.04	4.74	0
14	457.13	21.44	25.62	538.14	366.48	80.58	24.42
15	559.36	42.36	0	561.29	557.43	1.44	0
16	804.32	43.61	8.25	867.97	759.95	34.38	3.91
17	968.27	39.04	6.75	991.41	867.97	41.83	3.46
18	1082.07	4.82	28.14	1209.37	993.34	189.45	69.26
19	1236.37	15.8	6.28	1352.1	1209.37	77.23	-3.89
20	1454.33	42.3	0.46	1460.11	1442.75	6.44	0.05
21	1635.64	30.41	0.41	1637.56	1575.84	27.32	-0.24
22	2312.65	37.65	0.86	2337.72	2027.19	127.83	1.06
23	3450.65	8.72	12.16	3660.89	2364.73	847.92	87.99
24	3732.26	21.44	0.04	3734.19	3730.33	2.58	0

Comment;
MCM - 48 - 750

Date/Time; 4/22/2021 12:14:16 PM
No. of Scans;
Resolution;
Apodization;

Lampiran 8. Penentuan aktivitas katalis pada reaksi esterifikasi minyak nyamplung dengan menggunakan metode titrasi asam basa

- **Menggunakan katalis MCM-48/650**

Massa minyak yang digunakan= 2,75 g

Massa minyak yang diperoleh (produk) = 1,88 g

$$\text{Rendemen} = \frac{\text{Produk reaksi(g)}}{\text{Produk reaksi (g)}} \times 100\%$$

$$\text{Rendemen} = \frac{1{,}88 \text{ g}}{2{,}75 \text{ g}} \times 100\%$$

Rendemen = 68,36%

$$\text{Konversi} = \frac{(\text{FFA sebelum - FFA sesudah})}{\text{FFA sebelum}} \times 100\%$$

$$\text{Konversi} = \frac{(20{,}33\% - 9{,}70\%)}{20{,}33\%} \times 100\%$$

Konversi = 52,29%

$$\text{Aktivitas} = \frac{\text{Konversi (\%)}}{100\%} \times \text{Rendemen (\%)}$$

$$\text{Aktivitas} = \frac{52{,}29\%}{100\%} \times 68{,}36\%$$

Aktivitas = 35,74%

- **Perhitungan yang sama untuk semua aktivitas katalis di dalam penelitian ini. Kadar FFA diperoleh dari data titrasi asam basa yang dilakukan sebanyak tiga kali (triplo)**

Lampiran 9. Kromatogram GC-MS minyak nyamplung hasil esterifikasi menggunakan katalis MCM-48/650

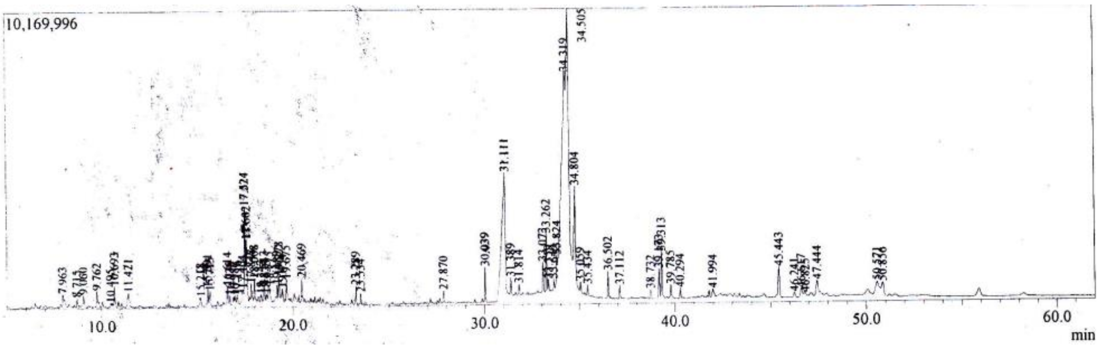

Lampiran 10. Hasil XRF CaO dari kulit telur ayam

```
SAMPLE ANALYSIS REPORT                                   THERMO FISHER SCIENTIFIC
ARL QUANT'X EDXRF ANALYZER                          UNIQUANT(TM) STANDARDLESS METHOD
_____________________________________________________________________________________
C:\UQed\USER\Quant'X\Job\JOB.588    2021-03-17
CaO#KT

Quant'X Rh end window 50kV
C:\UQed\USER\Quant'X\Appl\AnySampleAir.kap 2008-06-13
Calculated as :  Elements     Matrix (Shape & ImpFc) :  4|Ca..
X-ray path     =     Air      Film type     = No supporting film
Case number    =  0  All known
Eff.Diam.      = 13.0 mm      Eff.Area      = 132.7 mm2
KnownConc      =  0    %
Rest           =  0    %                    Viewed Mass    = 500.00 mg
Dil/Sample     =  0                         Sample Height = 5.00 mm

          El     m/m%     StdErr
          --    -------- -------
          Ca     99.66    0.15
          Px      0.257   0.034
          Nb      0.0255  0.0018
          Mo      0.0192  0.0016
          Ru      0.0081  0.0015

          In      0.0064  0.0009
          Sn      0.0063  0.0011
          Rh      0.0060  0.0014
          Sb      0.0052  0.0012

KnownConc= 0                  REST= 0                  D/S= 0
Sum Conc's before normalisation to 100% :   49.6 %

CaO#KT oks

Quant'X Rh end window 50kV
C:\UQed\USER\Quant'X\Appl\AnySampleAir.kap 2008-06-13
Calculated as :  Oxides       Matrix (Shape & ImpFc) :  4|Ca..
X-ray path     =     Air      Film type     = No supporting film
Case number    =  0  All known
Eff.Diam.      = 13.0 mm      Eff.Area      = 132.7 mm2
KnownConc      =  0    %
Rest           =  0    %                    Viewed Mass    =  500.000 mg
Dil/Sample     =  0                         Sample Height = 3.77 mm

          Compound m/m%    StdErr  | El     m/m%     StdErr
          ------ -------- ------- | --    -------- -------
          CaO     99.45    0.13   | Ca     71.11    0.09
          P2O5     0.478   0.062  | Px      0.209   0.027
          Nb2O5    0.0230  0.0016 | Nb      0.0161  0.0011
          MoO3     0.0182  0.0015 | Mo      0.0121  0.0010
          RuO4     0.0068  0.0013 | Ru      0.0052  0.0010

          SnO2     0.0051  0.0011 | Sn      0.0040  0.0008

KnownConc= 0                  REST= 0                  D/S= 0
Sum Conc's before normalisation to 100% :    58.8 %
Total % stripped Oxygen:  28.632
```

Lampiran 11. Data BET-BJH katalis MCM-48/550 dan ZMC/C/1:1/550

a. MCM-48/550

Sample: MCM-48/550
Operator: Sarah
Submitter: 24807
File: C:\TriStar II 3020\data\SAMPEL\2021\Desemb...\MCM-48-550.SMP

Started:	12/8/2021 7:03:43 AM	Analysis Adsorptive:	N2
Completed:	12/8/2021 4:18:28 PM	Analysis Bath Temp.:	-195.850 °C
Report Time:	12/9/2021 7:27:53 AM	Thermal Correction:	No
Sample Mass:	0.2000 g	Warm Free Space:	10.9805 cm³ Measured
Cold Free Space:	31.7812 cm³	Equilibration Interval:	5 s
Low Pressure Dose:	None	Sample Density:	1.000 g/cm³
Automatic Degas:	No		

Summary Report

Surface Area

Single point surface area at P/Po = 0.294141187: 1,058.3985 m²/g

BET Surface Area: 1,074.3386 m²/g

t-Plot External Surface Area: 1,079.6583 m²/g

BJH Adsorption cumulative surface area of pores between 1.7000 nm and 300.0000 nm diameter: 1361.324 m²/g

BJH Desorption cumulative surface area of pores between 1.7000 nm and 300.0000 nm diameter: 1,430.4852 m²/g

D-H Adsorption cumulative surface area of pores between 1.7000 nm and 300.0000 nm diameter: 1118.938 m²/g

D-H Desorption cumulative surface area of pores between 1.7000 nm and 300.0000 nm diameter: 1,380.4468 m²/g

b. ZMC/B/1:1/550

Sample:	KT 1:1/550
Operator:	Sarah
Submitter:	37341
File:	C:\TriStar II 3020\data\SAMPEL\2022\April\Samp...\KT 1-1.SMP

Started:	4/27/2022 7:23:30 AM	Analysis Adsorptive:	N2
Completed:	4/28/2022 6:32:43 AM	Analysis Bath Temp.:	-195.850 °C
Report Time:	4/28/2022 12:17:20 PM	Thermal Correction:	No
Sample Mass:	0.1269 g	Warm Free Space:	11.3900 cm³ Measured
Cold Free Space:	32.6031 cm³	Equilibration Interval:	5 s
Low Pressure Dose:	None	Sample Density:	1.000 g/cm³
Automatic Degas:	No		

Summary Report

Surface Area

Single point surface area at P/Po = 0.294463850:	932.4428 m²/g
BET Surface Area:	945.6838 m²/g
t-Plot External Surface Area:	1,012.2597 m²/g
BJH Adsorption cumulative surface area of pores between 1.7000 nm and 300.0000 nm diameter:	1096.254 m²/g
BJH Desorption cumulative surface area of pores between 1.7000 nm and 300.0000 nm diameter:	1,176.7836 m²/g
D-H Adsorption cumulative surface area of pores between 1.7000 nm and 300.0000 nm diameter:	1001.964 m²/g
D-H Desorption cumulative surface area of pores between 1.7000 nm and 300.0000 nm diameter:	1,158.7666 m²/g

Lampiran 12. Hasil XRF katalis CTAB-ZMC/A/1:1 dan CTAB-ZMC/B/1:1

a. CTAB-ZMC/A/1:1

```
SAMPLE ANALYSIS REPORT                              THERMO FISHER SCIENTIFIC
ARL QUANT'X EDXRF ANALYZER                  UNIQUANT(TM) STANDARDLESS METHOD
________________________________________________________________________________
C:\UQed\USER\Quant'X\Job\JOB.587    2021-03-17
CTA#ZML

Quant'X Rh end window 50kV
C:\UQed\USER\Quant'X\Appl\AnySampleAir.kap 2008-06-13
Calculated as :  Elements     Matrix (Shape & ImpFc) :  1|Teflon
X-ray path    =     Air       Film type     = No supporting film
Case number   =  0  All known
Eff.Diam.     = 13.0 mm       Eff.Area      = 132.7 mm2
KnownConc     =  0    %
Rest          =  0    %                     Viewed Mass    = 500.00 mg
Dil/Sample    =  0                          Sample Height = 5.00 mm

          El     m/m%     StdErr
          --     -------- -------
          Si      87.13    0.20
          Ca       7.46    0.13
          Zn       2.86    0.08
          Px       1.42    0.15
          Cl       0.63    0.17

          Br       0.495   0.025
          Zr       0.0087  0.0013

KnownConc= 0                 REST= 0                   D/S= 0
Sum Conc's before normalisation to 100% :   25.5 %
CTA#ZML oks

Quant'X Rh end window 50kV
C:\UQed\USER\Quant'X\Appl\AnySampleAir.kap 2008-06-13
Calculated as :  Oxides       Matrix (Shape & ImpFc) :  1|Teflon
X-ray path    =     Air       Film type     = No supporting film
Case number   =  0  All known
Eff.Diam.     = 13.0 mm       Eff.Area      = 132.7 mm2
KnownConc     =  0    %
Rest          =  0    %                     Viewed Mass    =  500.000 mg
Dil/Sample    =  0                          Sample Height = 3.77 mm

          Compound m/m%    StdErr  | El     m/m%     StdErr
          ------ -------- ------- | --     -------- -------
          SiO2    95.10    0.13   | Si      44.46    0.06
          CaO      3.17    0.09   | Ca       2.27    0.06
          ZnO      0.982   0.049  | Zn       0.789   0.039
          P2O5     0.41    0.12   | Px       0.179   0.054
          Cl       0.199   0.052  | Cl       0.199   0.052

          Br       0.131   0.007  | Br       0.131   0.007

KnownConc= 0                 REST= 0                   D/S= 0
Sum Conc's before normalisation to 100% :   49.8 %
Total % stripped Oxygen: 51.971
```

b. CTAB-ZMC/B/1:1

```
SAMPLE ANALYSIS REPORT                                      THERMO FISHER SCIENTIFIC
ARL QUANT'X EDXRF ANALYZER                           UNIQUANT(TM) STANDARDLESS METHOD
_____________________________________________________________________________________
C:\UQed\USER\Quant'X\Job\JOB.589    2021-03-17
CTA#ZMC#P

Quant'X Rh end window 50kV
C:\UQed\USER\Quant'X\Appl\AnySampleAir.kap 2008-06-13
Calculated as :  Elements      Matrix (Shape & ImpFc) :  1|Teflon
X-ray path     =    Air        Film type     = No supporting film
Case number    =  0  All known
Eff.Diam.      = 13.0 mm       Eff.Area      = 132.7 mm2
KnownConc      =  0    %
Rest           =  0    %                     Viewed Mass    = 500.00 mg
Dil/Sample     =  0                          Sample Height = 5.00 mm

          El      m/m%     StdErr
          --    -------- -------
          Si      84.02    0.19
          Ca       9.09    0.14
          Zn       3.76    0.10
          Br       1.46    0.06
          Px       1.12    0.13

          Cl       0.48    0.19
          Zr       0.0473  0.0056
          Nb       0.0094  0.0018

KnownConc= 0                   REST= 0                    D/S= 0
Sum Conc's before normalisation to 100% :    30.5 %
CTA#ZMC#P oks

Quant'X Rh end window 50kV
C:\UQed\USER\Quant'X\Appl\AnySampleAir.kap 2008-06-13
Calculated as :  Oxides        Matrix (Shape & ImpFc) :  1|Teflon
X-ray path     =    Air        Film type     = No supporting film
Case number    =  0  All known
Eff.Diam.      = 13.0 mm       Eff.Area      = 132.7 mm2
KnownConc      =  0    %
Rest           =  0    %                     Viewed Mass    =  500.000 mg
Dil/Sample     =  0                          Sample Height = 3.77 mm

          Compound m/m%    StdErr  | El      m/m%     StdErr
          ------ -------- -------  | --    -------- -------
          SiO2     93.50   0.12    | Si     43.71    0.06
          CaO       4.20   0.10    | Ca      3.00    0.07
          ZnO       1.39   0.06    | Zn      1.12    0.05
          Br        0.408  0.020   | Br      0.408   0.020
          P2O5      0.32   0.11    | Px      0.138   0.049

          Cl        0.161  0.065   | Cl      0.161   0.065
          ZrO2      0.0176 0.0021  | Zr      0.0130  0.0015

KnownConc= 0                   REST= 0                    D/S= 0
Sum Conc's before normalisation to 100% :    55.3 %
Total % stripped Oxygen: 51.444
```

Lampiran 13. Hasil karakterisasi menggunakan XRF untuk katalis CTAB-ZMC/B dalam berbagai variasi perndingan ZnO : CaO

a. CTAB-ZMC/B/1:0

```
SAMPLE ANALYSIS REPORT                                THERMO FISHER SCIENTIFIC
ARL QUANT'X EDXRF ANALYZER                    UNIQUANT(TM) STANDARDLESS METHOD
--------------------------------------------------------------------------------
C:\UQed\USER\Quant'X\Job\JOB.766    2021-08-19
1b0#Admin

Quant'X Rh end window 50kV
C:\UQed\USER\Quant'X\Appl\AnySampleAir.kap 2008-06-13
Calculated as :  Elements     Matrix (Shape & ImpFc) :  1|Teflon
X-ray path     =    Air       Film type      = No supporting film
Case number    =  0  All known
Eff.Diam.      = 13.0 mm      Eff.Area       = 132.7 mm2
KnownConc      =  0    %
Rest           =  0    %                     Viewed Mass    = 1000.00 mg
Dil/Sample     =  0                          Sample Height = 5.00 mm

          El      m/m%     StdErr
          --    -------- -------
          Si      71.95    2.06
          Zn      14.78    0.44
          Mg       9.58    2.30
          Br       3.24    0.10
          Px       0.349   0.100

          Zr       0.0533  0.0083
          Sr       0.0145  0.0028
          Nb       0.0123  0.0027
          In       0.0069  0.0006
          Sn       0.0056  0.0006


KnownConc= 0                   REST= 0                  D/S= 0
Sum Conc's before normalisation to 100% :    43.0 %
1b0#Admin oks

Quant'X Rh end window 50kV
C:\UQed\USER\Quant'X\Appl\AnySampleAir.kap 2008-06-13
Calculated as :  Oxides       Matrix (Shape & ImpFc) :  1|Teflon
X-ray path     =    Air       Film type      = No supporting film
Case number    =  0  All known
Eff.Diam.      = 13.0 mm      Eff.Area       = 132.7 mm2
KnownConc      =  0    %
Rest           =  0    %                     Viewed Mass    = 1000.000 mg
Dil/Sample     =  0                          Sample Height = 7.54 mm

          Compound m/m%    StdErr  | El      m/m%     StdErr
          ------ -------- -------  | --    -------- -------
          SiO2    91.31    0.14    | Si      42.69    0.07
          ZnO      7.51    0.13    | Zn       6.03    0.11
          Br       1.14    0.05    | Br       1.14    0.05
          Cl       0.044   0.022   | Cl       0.044   0.022
          ZrO2     0.0255  0.0031  | Zr       0.0189  0.0023

          Nb2O5    0.0061  0.0012  | Nb       0.0043  0.0008

KnownConc= 0                   REST= 0                  D/S= 0
Sum Conc's before normalisation to 100% :    63.9 %
Total % stripped Oxygen: 50.107
```

c. CTAB-ZMC/B/1:4

```
SAMPLE ANALYSIS REPORT                                  THERMO FISHER SCIENTIFIC
ARL QUANT'X EDXRF ANALYZER                         UNIQUANT(TM) STANDARDLESS METHOD
________________________________________________________________________________
C:\UQed\USER\Quant'X\Job\JOB.763    2021-08-19
1b4#admin

Quant'X Rh end window 50kV
C:\UQed\USER\Quant'X\Appl\AnySampleAir.kap 2008-06-13
Calculated as :  Elements     Matrix (Shape & ImpFc) :  1|Teflon
X-ray path     =    Air       Film type      = No supporting film
Case number    =  0  All known
Eff.Diam.      = 13.0 mm      Eff.Area       = 132.7 mm2
KnownConc      =  0    %
Rest           =  0    %                     Viewed Mass    = 1000.00 mg
Dil/Sample     =  0                          Sample Height = 5.00 mm

          El     m/m%     StdErr
          --     -------- -------
          Si      94.48    0.13
          Br       2.89    0.08
          Px       1.16    0.13
          Zn       0.974   0.049
          Ca       0.392   0.031

          Zr       0.0515  0.0060
          Sr       0.0197  0.0022
          Nb       0.0120  0.0010

KnownConc= 0                  REST= 0                  D/S= 0
Sum Conc's before normalisation to 100% :    35.1 %
1b4#admin oks

Quant'X Rh end window 50kV
C:\UQed\USER\Quant'X\Appl\AnySampleAir.kap 2008-06-13
Calculated as :  Oxides       Matrix (Shape & ImpFc) :  1|Teflon
X-ray path     =    Air       Film type      = No supporting film
Case number    =  0  All known
Eff.Diam.      = 13.0 mm      Eff.Area       = 132.7 mm2
KnownConc      =  0    %
Rest           =  0    %                     Viewed Mass    = 1000.000 mg
Dil/Sample     =  0                          Sample Height = 7.54 mm

          Compound m/m%    StdErr  | El     m/m%     StdErr
          ------ -------- -------  | --     -------- -------
          SiO2     98.45    0.09   | Si     46.02     0.04
          Br        0.781   0.039  | Br      0.781    0.039
          ZnO       0.339   0.017  | Zn      0.273    0.014
          P2O5      0.241   0.094  | Px      0.105    0.041
          CaO       0.159   0.012  | Ca      0.113    0.009

          ZrO2      0.0177  0.0019 | Zr      0.0131   0.0014

KnownConc= 0                  REST= 0                  D/S= 0
Sum Conc's before normalisation to 100% :    70.7 %
Total % stripped Oxygen: 52.679
```

d. CTAB-ZMC/B/1:8

```
SAMPLE ANALYSIS REPORT                                    THERMO FISHER SCIENTIFIC
ARL QUANT'X EDXRF ANALYZER                          UNIQUANT(TM) STANDARDLESS METHOD
____________________________________________________________________________________
C:\UQed\USER\Quant'X\Job\JOB.765    2021-08-19
1b8#adMin

Quant'X Rh end window 50kV
C:\UQed\USER\Quant'X\Appl\AnySampleAir.kap 2008-06-13
Calculated as :  Elements     Matrix (Shape & ImpFc) :  1|Teflon
X-ray path    =     Air       Film type     = No supporting film
Case number   =  0  All known
Eff.Diam.     = 13.0 mm       Eff.Area      = 132.7 mm2
KnownConc     =  0   %
Rest          =  0   %                      Viewed Mass   = 1000.00 mg
Dil/Sample    =  0                          Sample Height = 5.00 mm

          El     m/m%     StdErr
          --    -------- -------
          Si     68.53    1.72
          Zn     12.71    0.33
          Mg      8.52    2.06
          Ca      6.05    0.16
          Br      3.48    0.10

          Px      0.608   0.099
          Zr      0.0406  0.0079
          Sr      0.0402  0.0022
          Nb      0.0090  0.0021

KnownConc= 0                  REST= 0                    D/S= 0
Sum Conc's before normalisation to 100% :   47.3 %
1b8#adMin oks

Quant'X Rh end window 50kV
C:\UQed\USER\Quant'X\Appl\AnySampleAir.kap 2008-06-13
Calculated as :  Oxides       Matrix (Shape & ImpFc) :  1|Teflon
X-ray path    =     Air       Film type     = No supporting film
Case number   =  0  All known
Eff.Diam.     = 13.0 mm       Eff.Area      = 132.7 mm2
KnownConc     =  0   %
Rest          =  0   %                      Viewed Mass   = 1000.000 mg
Dil/Sample    =  0                          Sample Height = 7.54 mm

          Compound m/m%    StdErr  | El     m/m%     StdErr
          ------ -------- -------  | --    -------- -------
          SiO2    88.06    0.16    | Si     41.17    0.07
          ZnO      6.43    0.12    | Zn      5.17    0.10
          CaO      3.84    0.10    | Ca      2.75    0.07
          Br       1.26    0.06    | Br      1.26    0.06
          P2O5     0.37    0.10    | Px      0.162   0.044

          ZrO2     0.0197  0.0032  | Zr      0.0146  0.0023
          SrO      0.0119  0.0017  | Sr      0.0101  0.0015

KnownConc= 0                  REST= 0                    D/S= 0
Sum Conc's before normalisation to 100% :   69.6 %
Total % stripped Oxygen: 49.469
```

e. CTAB-ZMC/B/1: 16

```
SAMPLE ANALYSIS REPORT                                   THERMO FISHER SCIENTIFIC
ARL QUANT'X EDXRF ANALYZER                          UNIQUANT(TM) STANDARDLESS METHOD
_________________________________________________________________________________
C:\UQed\USER\Quant'X\Job\JOB.762    2021-08-19
admiN#1b16

Quant'X Rh end window 50kV
C:\UQed\USER\Quant'X\Appl\AnySampleAir.kap 2008-06-13
Calculated as :  Elements     Matrix (Shape & ImpFc) :  1|Teflon
X-ray path     =     Air      Film type     = No supporting film
Case number    =  0  All known
Eff.Diam.      = 13.0 mm      Eff.Area      = 132.7 mm2
KnownConc      =  0    %
Rest           =  0    %                    Viewed Mass    = 1000.00 mg
Dil/Sample     =  0                         Sample Height = 5.00 mm

          El      m/m%     StdErr
          --      -------- -------
          Si       86.96    0.16
          Zn        6.54    0.12
          Ca        2.65    0.08
          Br        2.00    0.07
          Px        1.76    0.14

          Sr        0.0345  0.0025
          Zr        0.0259  0.0047
          Nb        0.0078  0.0007

KnownConc= 0                  REST= 0                 D/S= 0
Sum Conc's before normalisation to 100% :   35.8 %
admiN#1b16 oks

Quant'X Rh end window 50kV
C:\UQed\USER\Quant'X\Appl\AnySampleAir.kap 2008-06-13
Calculated as :  Oxides       Matrix (Shape & ImpFc) :  1|Teflon
X-ray path     =     Air      Film type     = No supporting film
Case number    =  0  All known
Eff.Diam.      = 13.0 mm      Eff.Area      = 132.7 mm2
KnownConc      =  0    %
Rest           =  0    %                    Viewed Mass    = 1000.000 mg
Dil/Sample     =  0                         Sample Height = 7.54 mm

          Compound m/m%     StdErr  | El      m/m%     StdErr
          ------ -------- -------   | --      -------- -------
          SiO2     94.72    0.12    | Si       44.28    0.05
          ZnO       2.48    0.08    | Zn        2.00    0.06
          CaO       1.24    0.06    | Ca        0.885   0.040
          P2O5      0.98    0.11    | Px        0.430   0.049
          Br        0.552   0.028   | Br        0.552   0.028

          SrO       0.0107  0.0008  | Sr        0.0090  0.0007
          ZrO2      0.0094  0.0017  | Zr        0.0070  0.0012

KnownConc= 0                  REST= 0                 D/S= 0
Sum Conc's before normalisation to 100% :   63.8 %
Total % stripped Oxygen: 51.837
```

f. CTAB-ZMC/B/1: 32

```
1B32#admIn

Quant'X Rh end window 50kV
C:\UQed\USER\Quant'X\Appl\AnySampleAir.kap 2008-06-13
Calculated as :  Elements     Matrix (Shape & ImpFc) :  1|Teflon
X-ray path     =    Air       Film type     = No supporting film
Case number    =  0  All known
Eff.Diam.      = 13.0 mm      Eff.Area      = 132.7 mm2
KnownConc      =  0    %
Rest           =  0    %                    Viewed Mass    = 1000.00 mg
Dil/Sample     =  0                         Sample Height = 5.00 mm

          El      m/m%     StdErr
          --      -------- -------
          Si       89.97    0.19
          Ca        4.86    0.11
          Br        2.48    0.08
          Px        1.27    0.17
          Zn        0.890   0.045

          Fe        0.318   0.042
          Sr        0.132   0.007
          Zr        0.052   0.011
          Nb        0.0134  0.0012

KnownConc= 0                    REST= 0                    D/S= 0
Sum Conc's before normalisation to 100% :    33.2 %
1B32#admIn oks

Quant'X Rh end window 50kV
C:\UQed\USER\Quant'X\Appl\AnySampleAir.kap 2008-06-13
Calculated as :  Oxides       Matrix (Shape & ImpFc) :  1|Teflon
X-ray path     =    Air       Film type     = No supporting film
Case number    =  0  All known
Eff.Diam.      = 13.0 mm      Eff.Area      = 132.7 mm2
KnownConc      =  0    %
Rest           =  0    %                    Viewed Mass    = 1000.000 mg
Dil/Sample     =  0                         Sample Height = 7.54 mm

          Compound  m/m%   StdErr  | El      m/m%     StdErr
          ------ -------- ------- | --     -------- -------
          SiO2     96.04    0.12   | Si      44.90    0.06
          CaO       1.96    0.07   | Ca       1.40    0.05
          P2O5      0.87    0.12   | Px       0.381   0.052
          Br        0.644   0.032  | Br       0.644   0.032
          ZnO       0.296   0.015  | Zn       0.238   0.012

          Fe2O3     0.124   0.016  | Fe       0.087   0.011
          SrO       0.0349  0.0018 | Sr       0.0295  0.0015
          ZrO2      0.0177  0.0035 | Zr       0.0131  0.0026

KnownConc= 0                    REST= 0                    D/S= 0
Sum Conc's before normalisation to 100% :    67.6 %
Total % stripped Oxygen: 52.300
```

Lampiran 14. Data BET-BJH katalis CTAB-ZMC/B dalam berbagai variasi berbandingan ZnO : CaO

a. CTAB-ZMC/B/1: 0

Sample: KT-1:0
Operator: Sarah
Submitter: 24807
File: C:\TriStar II 3020\data\SAMPEL\2021\Desember\S...\KT-1-0.SMP

Started:	12/8/2021 7:03:43 AM	Analysis Adsorptive:	N2
Completed:	12/8/2021 4:18:29 PM	Analysis Bath Temp.:	-195.850 °C
Report Time:	12/9/2021 7:29:05 AM	Thermal Correction:	No
Sample Mass:	0.2817 g	Warm Free Space:	11.2049 cm³ Measured
Cold Free Space:	32.3262 cm³	Equilibration Interval:	5 s
Low Pressure Dose:	None	Sample Density:	1.000 g/cm³
Automatic Degas:	No		

Summary Report

Surface Area

Single point surface area at P/Po = 0.299126615: 853.2284 m²/g

BET Surface Area: 883.5099 m²/g

t-Plot External Surface Area: 1,443.6306 m²/g

BJH Adsorption cumulative surface area of pores between 1.7000 nm and 300.0000 nm diameter: 560.555 m²/g

BJH Desorption cumulative surface area of pores between 1.7000 nm and 300.0000 nm diameter: 437.7511 m²/g

D-H Adsorption cumulative surface area of pores between 1.7000 nm and 300.0000 nm diameter: 935.184 m²/g

D-H Desorption cumulative surface area of pores between 1.7000 nm and 300.0000 nm diameter: 967.8226 m²/g

b. CTAB-ZMC/B/1: 1

Sample:	KT-1:1
Operator:	Sarah
Submitter:	24807
File:	C:\TriStar II 3020\data\SAMPEL\2021\Desember\S...\KT-1-1.SMP

Started:	12/8/2021 7:03:43 AM	Analysis Adsorptive:	N2
Completed:	12/8/2021 4:18:29 PM	Analysis Bath Temp.:	-195.850 °C
Report Time:	12/9/2021 7:28:26 AM	Thermal Correction:	No
Sample Mass:	0.2757 g	Warm Free Space:	11.2174 cm³ Measured
Cold Free Space:	32.3916 cm³	Equilibration Interval:	5 s
Low Pressure Dose:	None	Sample Density:	1.000 g/cm³
Automatic Degas:	No		

Summary Report

Surface Area

Single point surface area at P/Po = 0.293296352:	939.1855 m²/g
BET Surface Area:	927.7177 m²/g
t-Plot External Surface Area:	1,775.4237 m²/g
BJH Adsorption cumulative surface area of pores between 1.7000 nm and 300.0000 nm diameter:	893.325 m²/g
BJH Desorption cumulative surface area of pores between 1.7000 nm and 300.0000 nm diameter:	895.6709 m²/g
D-H Adsorption cumulative surface area of pores between 1.7000 nm and 300.0000 nm diameter:	974.408 m²/g
D-H Desorption cumulative surface area of pores between 1.7000 nm and 300.0000 nm diameter:	1,035.8453 m²/g

c. CTAB-ZMC/B/1: 4

Sample: KT-1:4
Operator: Sarah
Submitter: 24807
File: C:\TriStar II 3020\data\SAMPEL\2021\Desember\S...\KT-1-4.SMP

Started:	12/9/2021 4:24:45 PM	Analysis Adsorptive:	N2
Completed:	12/10/2021 1:27:11 AM	Analysis Bath Temp.:	-195.850 °C
Report Time:	12/10/2021 6:38:36 AM	Thermal Correction:	No
Sample Mass:	0.2382 g	Warm Free Space:	11.1608 cm³ Measured
Cold Free Space:	32.6313 cm³	Equilibration Interval:	5 s
Low Pressure Dose:	None	Sample Density:	1.000 g/cm³
Automatic Degas:	No		

Summary Report

Surface Area

Single point surface area at P/Po = 0.301546117: 484.4815 m²/g

BET Surface Area: 499.4141 m²/g

t-Plot External Surface Area: 718.7467 m²/g

BJH Adsorption cumulative surface area of pores between 1.7000 nm and 300.0000 nm diameter: 359.312 m²/g

BJH Desorption cumulative surface area of pores between 1.7000 nm and 300.0000 nm diameter: 391.9379 m²/g

D-H Adsorption cumulative surface area of pores between 1.7000 nm and 300.0000 nm diameter: 496.056 m²/g

D-H Desorption cumulative surface area of pores between 1.7000 nm and 300.0000 nm diameter: 513.3537 m²/g

d. CTAB-ZMC/B/1: 8

Sample:	KT 1:8
Operator:	Sarah
Submitter:	37341
File:	C:\TriStar II 3020\data\SAMPEL\2022\April\Sa...\KT 1-8 R.SMP

Started:	4/28/2022 6:43:09 AM	Analysis Adsorptive:	N2
Completed:	4/28/2022 12:02:01 PM	Analysis Bath Temp.:	-195.850 °C
Report Time:	4/28/2022 12:17:59 PM	Thermal Correction:	No
Sample Mass:	0.1357 g	Warm Free Space:	11.2199 cm³ Measured
Cold Free Space:	31.5490 cm³	Equilibration Interval:	5 s
Low Pressure Dose:	None	Sample Density:	1.000 g/cm³
Automatic Degas:	No		

Summary Report

Surface Area

Single point surface area at P/Po = 0.298590771:	583.9780 m²/g
BET Surface Area:	616.7270 m²/g
t-Plot External Surface Area:	1,148.7922 m²/g
BJH Adsorption cumulative surface area of pores between 1.7000 nm and 300.0000 nm diameter:	317.611 m²/g
BJH Desorption cumulative surface area of pores between 1.7000 nm and 300.0000 nm diameter:	291.8019 m²/g
D-H Adsorption cumulative surface area of pores between 1.7000 nm and 300.0000 nm diameter:	639.334 m²/g
D-H Desorption cumulative surface area of pores between 1.7000 nm and 300.0000 nm diameter:	619.3616 m²/g

e. CTAB-ZMC/B/1: 16

Sample: KT-1:16
Operator: Sarah
Submitter: 24807
File: C:\TriStar II 3020\data\SAMPEL\2021\Desember\...\KT-1-16.SMP

Started:	12/9/2021 4:24:45 PM	Analysis Adsorptive:	N2
Completed:	12/10/2021 1:27:12 AM	Analysis Bath Temp.:	-195.850 °C
Report Time:	12/10/2021 6:39:23 AM	Thermal Correction:	No
Sample Mass:	0.2392 g	Warm Free Space:	11.2201 cm^3 Measured
Cold Free Space:	32.8096 cm^3	Equilibration Interval:	5 s
Low Pressure Dose:	None	Sample Density:	1.000 g/cm^3
Automatic Degas:	No		

Summary Report

Surface Area

Single point surface area at P/Po = 0.292920444: 418.3444 m^2/g

BET Surface Area: 433.0673 m^2/g

t-Plot External Surface Area: 582.9624 m^2/g

BJH Adsorption cumulative surface area of pores between 1.7000 nm and 300.0000 nm diameter: 327.850 m^2/g

BJH Desorption cumulative surface area of pores between 1.7000 nm and 300.0000 nm diameter: 350.0525 m^2/g

D-H Adsorption cumulative surface area of pores between 1.7000 nm and 300.0000 nm diameter: 450.502 m^2/g

D-H Desorption cumulative surface area of pores between 1.7000 nm and 300.0000 nm diameter: 455.3409 m^2/g

f. CTAB-ZMC/B/1: 32

Sample:	KT 1:32
Operator:	Sarah
Submitter:	37341
File:	C:\TriStar II 3020\data\SAMPEL\2022\April\Sam...\KT 1-32.SMP

Started:	4/27/2022 7:23:30 AM	Analysis Adsorptive:	N2
Completed:	4/28/2022 6:32:44 AM	Analysis Bath Temp.:	-195.850 °C
Report Time:	4/28/2022 12:18:32 PM	Thermal Correction:	No
Sample Mass:	0.1410 g	Warm Free Space:	11.3296 cm³ Measured
Cold Free Space:	32.2518 cm³	Equilibration Interval:	5 s
Low Pressure Dose:	None	Sample Density:	1.000 g/cm³
Automatic Degas:	No		

Summary Report

Surface Area

Single point surface area at P/Po = 0.301660919:	454.4818 m²/g
BET Surface Area:	466.3005 m²/g
t-Plot External Surface Area:	644.9747 m²/g
BJH Adsorption cumulative surface area of pores between 1.7000 nm and 300.0000 nm diameter:	374.207 m²/g
BJH Desorption cumulative surface area of pores between 1.7000 nm and 300.0000 nm diameter:	387.4093 m²/g
D-H Adsorption cumulative surface area of pores between 1.7000 nm and 300.0000 nm diameter:	458.986 m²/g
D-H Desorption cumulative surface area of pores between 1.7000 nm and 300.0000 nm diameter:	477.0864 m²/g

Lampiran 15. Hasil uji keasaman katalis CTAB-ZMC/B dalam berbagai variasi perndingan ZnO : CaO

✓ **Perhitungan keasaman katalis CTAB-ZMC/B/1: 0**

$$\text{Total asam} = \frac{(W_3 - W_2)}{(W_2 - W_1) \times \text{BM piridin}}$$

$$\text{Total asam} = \frac{(13{,}6929\ g - 13{,}6917\ g)}{(13{,}6917\ g\text{-}13{,}5917\ g) \times 0{,}0791}$$

$$\text{Total asam} = \frac{(13{,}6929\ g - 13{,}6917\ g)}{(13{,}6917\ g - 13{,}5917\ g) \times 0{,}0791\ g/mmol}$$

$$\text{Total asam} = \frac{0{,}0008\ g}{0{,}1\ g \times 0{,}0791\ g/mmol}$$

$$\text{Total asam} = \frac{0{,}0008\ g}{0{,}1\ g \times 0{,}0791\ g/mmol}$$

$$\text{Total asam} = \frac{0{,}0008\ g}{0{,}00791\ g^2/\ mmol}$$

Total asam = 0,949224 mmol/g

- ✓ Perhitungan yang sama digunakan untuk menghitung keasaman katalis yang ada di dalam tabel berikut :

Lampiran 16. Densitas dan viskositas

Tabel. Hasil perhitungan viskositas dan densitas minyak nyamplung HSA atau SPC sebelum dan sesudah diesterifikasi

Sampel	**FFA (%)**	**Densitas (kg/cm^3)**	**Viskositas (mm^2/det)**
Sebelum esterifikasi HSA	20,33	945	50,58
Setelah esterifikasi HSA	6,93	934	40,21
Sebelum esterifikasi SPC	22,43	945	50,47
Setelah esterifikasi SPC	9,31	927	41,22

✓ Contoh perhitungan untuk minyak nyamplung HSA sebelum esterifikasi. Perhitungan yang sama untuk viskositas dan densitas semua minyak di dalam tabel.

a. Pengukuran densitas

1. Berat piknometer kosong (G_o) = 16,0657 g
2. Berat piknometer dan sampel pada suhu 40^{o}C (G) = 25,5015 g
3. Volume sampel pada suhu 40^{o}C (V_t) = 10 mL

$$\text{Densitas sampel} = \frac{\text{G} - \text{G}_\text{o}}{\text{V}_\text{t}} + 0{,}0012$$

$$\text{Densitas sampel} = \frac{25{,}5015\ \text{g} - 16{,}0657\ 8\ \text{g}}{10\ \text{mL}} + 0{,}0012$$

$$\text{Densitas sampel} = 0{,}94478\ \text{g/cm}^3$$

b. Pengukuran Viskositas

Pengukuran viskositas minyak nyamplung HSA sebelum esterifikasi yaitu menggunakan viskometer Ostwald pada suhu 40^{o}C dengan rincian sebagai berikut :

Pengukuran	**Waktu alir sampel (det)**	**Waktu alir akuades (det)**
I	4005,7	51,21
II	3937,83	51,21
III	4005,72	51,21
Rata-rata	3983,083	51,21

Dimana :

ρ_{sampel} (40^{o}C) = 0,94478 g/cm^3

$\rho_{akuades}$ (40^{o}C) = 1,00414 g/cm^3

$\pi_{akuades}$ (40^{o}C) = 0,00653 g/cm det

Perhitungan :

$$\pi_{Sampel} = \frac{\rho_{sampel\ x\ t_{sampel}}}{\rho_{akuades\ x\ t_{akuades}}} \text{ x } \pi_{akuades}$$

$$\pi_{Sampel} = \frac{0{,}94478 \text{ g cm}^{-3} \text{ x } 3983{,}083 \text{ det}}{1{,}00414 \text{ g cm}^{-3} \text{ x } 51{,}21 \text{ det}} \text{ x } 0{,}00653 \text{ g cm}^{-1} \text{ det}^{-1}$$

$$\pi_{Sampel} = \frac{3762{,}819 \text{ g cm}^{-3}\text{det}}{51{,}422 \text{ g cm}^{-3} \text{ det}} \text{ x } 0{,}00654 \text{ g cm}^{-1} \text{ det}^{-1}$$

$$\pi_{Sampel} = 73{,}175 \text{ x } 0{,}00653 \text{ g cm}^{-1} \text{ det}^{-1}$$

$$\pi_{Sampel} = 0{,}478 \text{ g cm}^{-1} \text{ det}^{-1}$$

$$V_{Sampel} = \frac{\pi_{Sampel}}{\rho_{sampel}}$$

$$V_{Sampel} = \frac{0{,}478 \text{ g cm}^{-1} \text{ det}^{-1}}{0{,}94478 \text{ g cm}^{-3}}$$

$$V_{Sampel} = 0{,}50576 \text{ cm}^2 \text{ det}^{-1}$$

$$V_{Sampel} = 50{,}58 \text{ mm}^2 \text{ det}^{-1}$$